Sparse Factor Analysis for Categorical Data with the Group-Sparse Generalized Singular Value Decomposition

Ju-Chi Yu, Julie Le Borgne, Anjali Krishnan, Arnaud Gloaguen, Cheng-Ta Yang, Laura A Rabin, Hervé Abdi, Vincent Guillemot

Sparse Factor Analysis for Categorical Data with the Group-Sparse Generalized Singular Value Decomposition

Ju-Chi Yu[a,*], Julie Le Borgne[b], Anjali Krishnan[c], Arnaud Gloaguen[d], Cheng-Ta Yang[e,f,g], Laura A. Rabin[c], Hervé Abdi[h,1,*], Vincent Guillemot[i,1,*]

[a] *Campbell Family Mental Health Research Institute, Centre for Addiction and Mental Health, Toronto, Canada*
[b] *Université de Lille, INSERM, CHU Lille, institut Pasteur Lille, U1167-riD-AGE, Facteurs de risque et déterminants moléculaires des maladies liées au vieillissement, Lille, France*
[c] *Department of Psychology, Brooklyn College of the City University of New York, BrookBlyn, USA*
[d] *Centre National de Recherche en Génomique Humaine (CNRGH), Institut de Biologie François Jacob, CEA, Université Paris-Saclay, Évry, France.*
[e] *Department of Psychology, National Cheng Kung University, Tainan, Taiwan*
[f] *Graduate Institute Mind, Brain and Consciousness, Taipei Medical University, Taipei, Taiwan*
[g] *Graduate Institute of Health and Biotechnology Law, Taipei Medical University, Taipei City, Taiwan*
[h] *The University of Texas at Dallas, Richardson, TX, USA*
[i] *Institut Pasteur, Université Paris Cité, Bioinformatics and Biostatistics Hub, F-75015 Paris, France*

Abstract

Correspondence analysis, multiple correspondence analysis and their discriminant counterparts (i.e., discriminant simple correspondence analysis and discriminant multiple correspondence analysis) are methods of choice for analyzing multivariate categorical data. In these methods, variables are integrated into optimal components computed as linear combinations whose weights are obtained from a generalized singular value decomposition (GSVD) that integrates specific metric constraints on the rows and columns of the original data matrix. The weights of the linear combinations are, in turn, used to interpret the components, and this interpretation is facilitated when components are 1) pairwise orthogonal and 2) when the values of the weights are either large or small but not intermediate—a pattern called a simple or a sparse structure. To obtain such simple configurations, the optimization problem solved by the GSVD is extended to include new constraints that implement component orthogonality and sparse weights. Because multiple correspondence analysis represents qualitative variables by a set of binary variables, an additional group constraint is added to the optimization problem in order to sparsify the whole set representing one qualitative variable. This new algorithm—called group-sparse GSVD (gsGSVD)—integrates these constraints via an iterative projection scheme onto the intersection of subspaces where each subspace implements a specific constraint. In this paper, we expose this new algorithm and show how it can be adapted to the sparsification of simple and multiple correspondence analysis, and illustrate its applications with the analysis of four different data sets—each illustrating the sparsification of a particular CA-based analysis.

Keywords: Sparsification, Multivariate Analysis, Correspondence Analysis, Discriminant Correspondence Analysis,

*Corresponding authors
Email addresses: Ju-Chi.Yu@camh.ca (Ju-Chi Yu), herve@utdallas.edu (Hervé Abdi), vincent.guillemot@pasteur.fr (Vincent Guillemot)
[1] Authors contributed equally

1. Introduction

In contemporary research, data sets routinely describe vast samples of observations (in the hundreds of thousands) with a large number of variables (in the millions or more) that can be quantitative, qualitative, or mixtures of these two data types. While principal component analysis (PCA) extracts components from quantitative data, typical component methods for qualitative data are correspondence analysis (CA) and multiple correspondence analysis (MCA, a generalization of CA). Like PCA, CA and MCA extract components that summarize the associations between qualitative variables by representing each variable with a set of binary columns corresponding to its levels ——a coding scheme called *disjunctive coding* or *group coding* in multivariate statistics, or *one hot encoding* in machine learning (see, e.g., Abdi et al., 2024).

Component methods create new variables (i.e., the *components*) obtained as linear combinations of the original variables, which optimally represent, on the one hand, the similarity structure of the observations by maps of the component space where the distance between observations approximates their similarity, and, on the other hand, the correlational structure of the variables by maps where the configuration of the variable levels approximates their covariance. Components——being linear combinations of the original variables—are often interpreted in terms of these variables and are easy to interpret when each component is obtained from a small number of variables where each variable only contributes to few (ideally one) components. Such a configuration is called a *simple* structure (Cattell, 1978; Thurstone, 1935)—a concept first elaborated for factor analysis methods by psychometricians (specifically "factorialists" such as, e.g., Thurstone, 1935; Cattell, 1978). By contrast, when the structure is not simple, components are hard to interpret because the contributing variables are hard to identify. To reach a simple solution and facilitate the interpretation of components, these early factorialists (Thurstone, 1935, 1947) developed heuristic procedures such as rotation. These procedures often simplify the interpretation (but at the cost of losing optimality and also sometimes orthogonality), particularly when the data fit the factorial hypotheses (e.g., a signal comprising a mixture of few well-defined orthogonal dimensions and independent additive Gaussian noise), but large data sets collected without a clear construct are unlikely to naturally have a simple structure recoverable from standard rotation procedures (Cattell, 1978). However, rotation is rarely (if ever) used to facilitate interpretation in the correspondence analysis family as MCA originated as a descriptive method (with data unlikely to follow the factorialist model), but finding simple structures has recently become more relevant because of the large size of modern data sets.

Another traditional approach (see, e.g., Saporta, 2011; Abdi and Béra, 2014) selects, for further investigation, items (i.e., rows or columns) whose contributions exceed the average contribution (i.e., the inverse of the number of items), or exceed their a priori mass when the items have different masses (i.e., such as in CA). These descriptive approaches can be complemented by some inferential procedures such as test values (a cousin of Student's t statistics, see, e.g., Lebart et al., 1984). More recently, computer-based resampling techniques (e.g., bootstrap, permutation)

provide non-parametric equivalents—such as bootstrap ratios—to these test values.

By contrast with these earlier heuristics, *sparsification*—the modern approach to "simplification"—which originated in a multiple regression framework, reframes simplification as an optimization problem whose goal is to minimize the sum of squared residuals while simultaneously minimizing the sum of the absolute values of the coefficients (a procedure originally called *least absolute shrinkage and selection operator*, better known as LASSO, see, Hastie et al., 2009; Journée et al., 2010; Efron and Hastie, 2016). In this context, when a model is sparsified, loadings below a specific threshold are shrunken to zero and so are eliminated from the model. Often, these redundant variables provide little *specific* information, and eliminating them from the model makes the prediction more reliable and easier to interpret (Efron, 2020). In the early 2000's, LASSO based sparsification methods have been extended to component methods, such as principal component analysis (PCA, see, e.g., Jolliffe and Uddin 2000; Jolliffe et al. 2003; Zou et al. 2006; Trendafilov 2014, for a recent review see, Trendafilov and Gallo 2021, Chapter 4). Both sparsification and rotation try to find a compromise between simplicity and amount of variance explained by the components. When used for PCA, sparsification appears as an alternative to rotation but, as argued by Trendafilov and Adachi (2015), sparsification is to be preferred because 1) for big data analysis, ease of interpretation should be prioritized over maximizing explained variance; and 2) concluding that small loadings obtained after a rotation are negligible can be misleading as the rotated dimensions are interpreted by imposing an arbitrary threshold and subjectively neglecting the loadings below this threshold (as illustrated by Cadima and Jolliffe, 1995).

Recently, several LASSO-based sparsification methods have been developed that be classified in three main approaches: 1) the $\mathcal{L}_1$ sparsification (i.e., the LASSO, per se, Tibshirani, 1996), 2) the $\mathcal{L}_\mathcal{G}$ group sparsification (i.e., the Group-LASSO, Yuan and Lin, 2006), and 3) the elastic net which combines $\mathcal{L}_1$ and $\mathcal{L}_2$ (Zou and Hastie, 2005). These sparsification methods concurrently maximize explained variance while penalizing (i.e., reducing or eliminating) non-zero, intermediate loadings. In practice, sparsification is implemented by adding specific constraints to the component maximization problem.

Existing sparsification methods are largely dominated by extensions of the penalized matrix decomposition (PMD) introduced by Witten et al. (2009) and by sparse PCA from Mackey (2009). However, very few sparse versions of CA and MCA have been developed. Notably, an early version of sparse MCA was introduced by Bernard et al. (2012), whose methodology was grounded in Witten et al. (2009)'s PMD. However, Bernard et al. (2012)'s approach did not rely on an explicit optimization problem nor did it guarantee the orthogonality of the resulting components. In a similar vein, Mori et al. (2016) proposed an alternative version of sparse MCA, based on an iterative algorithm that implements a decomposition of the dataset as an optimization problem under constraints, including orthogonality of loadings and sparsity. However, this method is mostly a heuristic because there is no convergence proof to indicate that this algorithm solves the optimization problem (note that as of 2023, the software associated with this publication is no longer available). In a very recent major advance, Liu et al. (2023) presented the first genuine sparse CA method rooted in PMD. In contrast with previous methods, Liu et al. include a deflation step (i.e., BiOPD) to *** HA *** minimize the correlation between components (but cannot guarantee true orthogonality, because sparsification is not

a linear problem).

These recent sparse methods sacrifice orthogonality for sparsity, because it is difficult to concurrently implement orthogonal components or orthogonal loadings (see, Journée et al. 2010; Trendafilov 2014; exceptions are Trendafilov and Jolliffe 2006, Qi et al. 2013, and Jolliffe et al. 2003 that can satisfy one of the constraints, but not both simultaneously). To maintain orthogonality with sparsification, Guillemot et al. (2019) developed a new SVD algorithm (called the constrained SVD, CSVD), which extends PMD to sparsify loadings and preserves orthogonality. Specifically, the CSVD imposes sparsification and orthogonality constraints by re-framing these constraints as convex spaces to solve the maximization problem by projecting the data onto the intersection of these spaces.

In this paper, we extend the CSVD to sparsify CA-related methods while maintaining the orthogonality of both components and factor scores. To do so, we extended the CSVD algorithm to incorporate 1) the metric matrices specific to CA and MCA and 2) group constraints necessary for MCA (because variables in MCA are represented by blocks of binary variables). Note that these group constraints can also be applied to groups of rows in CA or MCA. In this paper, we show how the CSVD can be applied to sparsifying CA and MCA and also to the barycentric discriminant analysis (Abdi, 2007) versions of CA (DiSCA) and MCA (DiMCA).

In the following sections, we show how group sparsity can be used for CA-based methods, which properties are kept or lost, and how to compute optimal values for the sparsity parameters. We illustrate these procedures with four examples (one per method). The reproducible R code of the methods and these examples are accessible online at `https://github.com/juchiyu/SPAFAC`.

2. Notations

Bold uppercase letters (e.g., $\mathbf{A}$) denote a matrix, bold lowercase letters (e.g., $\mathbf{a}$) denote a vector, and italic lowercase letters (e.g., a) denote the elements of a matrix or of a vector; the indices for elements of a set are denoted by italic lowercase letters (e.g., n) and the cardinal of a set by an italic uppercase letter (e.g., N). The matrix $\mathbf{I}$ is the identity matrix, $\mathbf{1}$ is a matrix of ones, and $\mathbf{0}$ a matrix of zeros (the dimensions of these matrices depend upon the context and are assumed to be conformable). The transpose operation for a matrix is denoted by the superscript $^\top$ (e.g., $\mathbf{A}^\top$) and the inverse of a square matrix (say $\mathbf{S}$) is denoted by the superscript $^{-1}$ (e.g., $\mathbf{S}^{-1}$). For a given data table, (except if stated otherwise) the number of rows is denoted I, and the number of columns is denoted J. The element stored in the ith row and jth column of matrix $\mathbf{X}$ is denoted $x_{i,j}$. For an $I \times J$ matrix, the minimum of I and J is the largest possible *rank*, denoted L, of the matrix. The actual rank of a matrix is denoted by R (with $R \leq L$). The operator $\mathsf{diag}\,()$ applied to a (square) matrix gives a vector with all elements on the diagonal of this matrix [i.e., $\mathsf{diag}\,(\mathbf{X}) = \mathbf{x}$, with $x_i = x_{i,i}$] and when applied to a vector, $\mathsf{diag}\,()$ gives a diagonal matrix with the elements of this vector on the diagonal and 0s elsewhere [i.e., $\mathbf{X} = \mathsf{diag}\,(\mathbf{x})$, with $x_i = x_{i,i}$ and $x_{i,j} = 0$ when $i \neq j$]. The operator $\mathsf{trace}\,(.)$ applied to a (square) matrix gives the sum of all diagonal elements of this matrix. The sum of squares of all elements of $\mathbf{X}$ is called the *inertia* of $\mathbf{X}$ and is equal to $\mathsf{trace}\left(\mathbf{X}^\top\mathbf{X}\right)$ and $\mathsf{trace}\left(\mathbf{X}\mathbf{X}^\top\right)$. The Hadamar (i.e., element-wise) product between two matrices of same dimensions is denoted $\odot$ (i.e., $\mathbf{A} \odot \mathbf{B}$).

The operator $\arg\max_{\mathbf{x}}(f(\mathbf{x}))$ identifies the argument $\mathbf{x}$ that maximizes the value of $f(\mathbf{x})$. Similarly, the operator $\arg\min_{\mathbf{x}}(f(\mathbf{x}))$ identifies the argument $\mathbf{x}$ that minimizes $f(\mathbf{x})$. The $\mathcal{L}_1$ norm of vector $\mathbf{a}$ is denoted by $\|\mathbf{a}\|_1$, and is computed as the sum of all absolute values of elements of $\mathbf{a}$; the $\mathcal{L}_2$ norm of vector $\mathbf{a}$, denoted by $\|\mathbf{a}\|_2$, is computed as $\sqrt{\mathbf{a}^\top\mathbf{a}}$. In the framework of the CSVD, additional notations are needed. The orthogonal complement of $\mathbf{A}$ is denoted by the superscript $^\perp$ (e.g., $\mathbf{A}^\perp$) and is the vector space of all the vectors orthogonal to the space spanned by $\mathbf{A}$. The space that contains all the vectors with an $\mathcal{L}_1$ norm inferior to s is called an $\mathcal{L}_1$-ball, and is denoted by $\mathscr{B}_1(s)$, with s defining the radius of the $\mathcal{L}_1$-ball. The space that contains all the vectors with an $\mathcal{L}_2$ norm inferior to s is called an $\mathcal{L}_2$-ball; and is denoted by $\mathscr{B}_2(s)$, with s defining the radius of the $\mathcal{L}_2$-ball. See also Appendix B for notation specific to the GSVD.

3. Method

CA-related methods use the generalized singular value decomposition (GSVD) to compute their components. Therefore, to sparsify these methods, we developed a sparsification algorithm for the GSVD, called the sparse GSVD (sGSVD; Yu et al., 2023). Further, as some CA-related methods analyze categorical data with qualitative variable being represented by groups of (binary) columns, we also extended the sGSVD to create the group-sparse GSVD (gsGSVD) that, in addition, performs group sparsification where pre-defined groups of columns or rows are kept or eliminated together. In the following sections, we first present the optimization problem of the gsGSVD, and the algorithm we developed to solve it. Next, we show how to applied the gsGSVD to sparsify CA, DiSCA, MCA, and DiMCA.

3.1. The group-sparse generalized SVD (gsGSVD)

To sparsify variables as groups of levels for CA-related methods, we extend the algorithm of the sGSVD to develop the group-sparse generalized SVD (gsGSVD), which sparsifies the elements of the generalized singular vectors of a given matrix $\mathbf{X}$ taking into account group constraints (on rows and columns) and constraints imposed by a metric matrix (denoted by $\mathbf{M}$) for the rows and a metric matrix (denoted by $\mathbf{W}$) for the columns (see Algorithm 1). Specifically, the gsGSVD maximization problem is expressed as:

$$\arg\max_{\mathbf{p}_\ell,\mathbf{q}_\ell}\left(\hat{\delta}_\ell = \mathbf{p}_\ell^\top\mathbf{M}^{\frac{1}{2}}\mathbf{X}\mathbf{W}^{\frac{1}{2}}\mathbf{q}_\ell\right) \quad \text{subject to}$$

$$\mathbf{p}_\ell \in \begin{cases} \mathscr{B}_{\mathcal{L}_2}(1) \\ \mathscr{B}_{\mathcal{G}_\mathbf{p}}(s_{\mathbf{p},\ell}) \\ \mathbf{P}_\ell^\perp \end{cases}, \qquad \mathbf{q}_\ell \in \begin{cases} \mathscr{B}_{\mathcal{L}_2}(1) \\ \mathscr{B}_{\mathcal{G}_\mathbf{q}}(s_{\mathbf{q},\ell}) \\ \mathbf{Q}_\ell^\perp \end{cases} \tag{1}$$

with respect to three constraints, involving: 1) the $\mathcal{L}_2$-ball that normalizes the singular vectors, 2) the orthogonal space (i.e., $\mathbf{P}_\ell^\perp$ or $\mathbf{Q}_\ell^\perp$) that ensures orthogonality between components, and 3) the $\mathcal{L}_\mathcal{G}$-ball that sparsifies the elements

of the (generalized) singular vectors in groups. The ℓth generalized pseudo-singular vector of $\mathbf{X}$ are then computed as $\mathbf{u}_\ell = \mathbf{M}^{-\frac{1}{2}}\mathbf{p}_\ell$ and $\mathbf{v}_\ell = \mathbf{W}^{-\frac{1}{2}}\mathbf{q}_\ell$. We solve this maximization problem by modifying the algorithm of the sGSVD (see Algorithm 1; cf. Algorithm E.4 in Appendix F), where the three constraints are implemented with the Projection Onto Convex Sets (POCS) procedure (Combettes, 1993). Specifically, the projection onto the $\mathcal{L}_2$-ball is equivalent to imposing constraints on the $\mathcal{L}_2$-norm, and the projection onto the $\mathcal{L}_\mathcal{G}$-norm ball is equivalent to imposing constraints on the group norm—defined as: $\|\mathbf{x}\|_\mathcal{G} = \sum_{g=1}^{G} \left\|\mathbf{x}_{\iota_g}\right\|_2$ (van den Berg et al., 2008). This group norm—called "the [1,2]-group norm" in van den Berg et al. (2008)—is the $\mathcal{L}_1$-norm of the vector containing the $\mathcal{L}_2$-norm of the sub-vectors defined by the groups. In this paper, we call this group norm the $\mathcal{L}_\mathcal{G}$-norm and its associated space the $\mathcal{L}_\mathcal{G}$-ball, denoted $\mathscr{B}_{\mathcal{G},}(\cdot)$. Finally, we reorder the dimensions in a decreasing order of the derived pseudo-singular values ($\hat{\delta}_\ell$). This final step is necessary because, as is the case for the sparse SVD, there is no guarantee that the gsGSVD will estimate the pseudo-singular values in a predefined order, especially when the sparsity constraint is strong.

3.2. Sparse CA and related methods

In this paper, we present four sparse CA-related methods: 1) CA, 2) MCA, and their discriminant analysis versions 3) DiSCA and 4) DiMCA. These methods are all specific cases of the gsGSVD, because they all use metric matrices and, in some cases, incoporate group structures on rows or columns. For example, CA (and DiSCA) analyzes a contingency table and includes metric matrices for both rows and columns, whereas MCA (and DiMCA) analyzes categorical variables with disjunctive coding and thus, additionally, takes into account a group structure on the columns. In the following sections, we expose the algorithms for each method as specific cases of the gsGSVD.

3.2.1. CA and sparse CA (sCA): sparsification with metric matrices

CA analyzes an I by J contingency table (denoted $\mathbf{A}$) by first deriving its probability matrix (denoted by $\mathbf{Z}$). To do so, given N observations (i.e., the grand total of $\mathbf{A}$), $\mathbf{Z}$ is computed as:

$$\mathbf{Z} = \frac{1}{N}\mathbf{A}. \tag{2}$$

To analyze the pattern of association between rows and columns, CA first computes the deviation from independence for $\mathbf{Z}$:

$$\mathbf{X} = \mathbf{Z} - \mathbf{r}\mathbf{c}^\top, \quad \text{where} \qquad \mathbf{r} = \mathbf{Z}\mathbf{1} \quad \text{and} \quad \mathbf{c} = \mathbf{Z}^\top\mathbf{1}. \tag{3}$$

Here, $\mathbf{r}$, respectively $\mathbf{c}$, stores the sums of the rows and the columns of $\mathbf{Z}$. Therefore, taking this deviation from independence is equivalent to centering both the rows and the columns of $\mathbf{Z}$ (i.e., *double-centering* $\mathbf{Z}$). CA then decomposes this double centered probability matrix $\mathbf{X}$ into 3 matrices by the GSVD:

$$\mathbf{X} = \mathbf{U}\boldsymbol{\Delta}\mathbf{V}^\top \quad \text{under the constraints} \quad \mathbf{U}^\top\mathbf{D}_\mathbf{r}^{-1}\mathbf{U} = \mathbf{V}^\top\mathbf{D}_\mathbf{c}^{-1}\mathbf{V} = \mathbf{I}, \tag{4}$$

Algorithm 1: General algorithm of group-sparse GSVD of $\mathbf{X}$

Data: $\mathbf{X}$
ε (error), R (rank, > 1),
$\mathbf{M}$ and $\mathbf{W}$ (row and column metric matrices),
$s_{\mathbf{p},\ell}$ and $s_{\mathbf{q},\ell}$ (sparse parameters for singular vectors),
$\mathcal{G}_{\mathbf{p}}$, and $\mathcal{G}_{\mathbf{q}}$ (group arrangements of rows and columns)
Result: group-sparse GSVD of $\mathbf{X}$
$\widetilde{\mathbf{X}} = \mathbf{M}^{\frac{1}{2}}\mathbf{X}\mathbf{W}^{\frac{1}{2}}$
$\mathbf{P} \leftarrow \mathbf{Q} \leftarrow \mathbf{U} \leftarrow \mathbf{V} \leftarrow \emptyset$; ▷ $\mathbf{P}$ and $\mathbf{Q}$ store the left and right pseudo-singular vectors
▷ $\mathbf{U}$ and $\mathbf{V}$ store the *generalized* left and right pseudo-singular vectors

for $\ell = 1, \ldots, R$ **do**
  Initialize $\mathbf{p}^{(0)}$ and $\mathbf{q}^{(0)}$ ▷ Initialize $\mathbf{p}$ and $\mathbf{q}$ either from SVD or randomly
  $\hat{\delta}^{(0)} \leftarrow \mathbf{p}^{(0)\top}\widetilde{\mathbf{X}}\mathbf{q}^{(0)}$ ▷ Initialize $\hat{\delta}$ with $\mathbf{p}^{(0)}$ and $\mathbf{q}^{(0)}$
  $t \leftarrow 0$
  while $\left(\left\|\mathbf{p}^{(t+1)} - \mathbf{p}^{(t)}\right\|_2 \geq \varepsilon\right)$ or $\left(\left\|\mathbf{q}^{(t+1)} - \mathbf{q}^{(t)}\right\|_2 \geq \varepsilon\right)$ **do**
    $\mathbf{p}^{(t+1)} \leftarrow \text{proj}(\ \widetilde{\mathbf{X}}\mathbf{q}^{(t)}, \mathscr{B}_{\mathcal{G}_{\mathbf{p}}}(s_{\mathbf{p},\ell}) \cap \mathscr{B}_{\mathcal{L}_2}(1) \cap \mathbf{P}^{\perp})$
    $\mathbf{q}^{(t+1)} \leftarrow \text{proj}(\ \widetilde{\mathbf{X}}^{\top}\mathbf{p}^{(t+1)}, \mathscr{B}_{\mathcal{G}_{\mathbf{q}}}(s_{\mathbf{q},\ell}) \cap \mathscr{B}_{\mathcal{L}_2}(1) \cap \mathbf{Q}^{\perp})$
    $\hat{\delta}^{(t+1)} \leftarrow \mathbf{p}^{(t+1)\top}\widetilde{\mathbf{X}}\mathbf{q}^{(t+1)}$
    $t \leftarrow t + 1$ ▷ Iterate until $\mathbf{p}$ and $\mathbf{q}$ are stable
  $\hat{\delta}_\ell \leftarrow \hat{\delta}^{(t)}$; $\mathbf{p}_\ell \leftarrow \mathbf{p}^{(t)}$; $\mathbf{q}_\ell \leftarrow \mathbf{q}^{(t)}$ ▷ $\mathbf{p}_\ell$ and $\mathbf{q}_\ell$ are the left and right pseudo-singular vectors of $\widetilde{\mathbf{X}}$

  $\mathbf{u}_\ell \leftarrow \mathbf{M}^{-\frac{1}{2}}\mathbf{p}_\ell$
  $\mathbf{v}_\ell \leftarrow \mathbf{W}^{-\frac{1}{2}}\mathbf{q}_\ell$ ▷ $\mathbf{u}_\ell$ and $\mathbf{v}_\ell$ are the left and right generalized pseudo-singular vectors of $\mathbf{X}$

  $\mathbf{P} \leftarrow [\,\mathbf{P} \mid \mathbf{p}_\ell\,]$; $\mathbf{Q} \leftarrow [\,\mathbf{Q} \mid \mathbf{q}_\ell\,]$
  $\mathbf{U} \leftarrow [\,\mathbf{U} \mid \mathbf{u}_\ell\,]$; $\mathbf{V} \leftarrow [\,\mathbf{V} \mid \mathbf{v}_\ell\,]$
Define $\widehat{\boldsymbol{\delta}} = (\hat{\delta}_1, \cdots, \hat{\delta}_R)$
Reorder $\widehat{\boldsymbol{\delta}}$ in decreasing order of its elements
$\widehat{\boldsymbol{\Delta}} \leftarrow \mathsf{diag}\left(\widehat{\boldsymbol{\delta}}\right)$
Reorder the columns of $\mathbf{U}$ and $\mathbf{V}$ according to $\widehat{\boldsymbol{\delta}}$

Note: The text colored in red is the sparsification constraints of the CSVD that are also used in the gsGSVD; the text colored in green is the metric constraints of the GSVD that are also used in the gsGSVD; and the text colored in blue is the group constraints that are specific to the gsGSVD.

where $\mathbf{D}_{\mathbf{r}} = \mathsf{diag}\,(\mathbf{r})$, $\mathbf{D}_{\mathbf{c}} = \mathsf{diag}\,(\mathbf{c})$. In this GSVD, the metric matrix $\mathbf{D}_{\mathbf{r}}^{-1}$ stores the row weights of $\mathbf{X}$, and the metric $\mathbf{D}_{\mathbf{c}}^{-1}$ stores the column weights of $\mathbf{X}$. With these metric matrices, CA gives the optimal decomposition for a given rank of the χ^2 associated to the contingency table $\mathbf{A}$ (see Appendix A). In addition, this GSVD is equivalent to the SVD of Equation B.5 and solves the same maximization problem (cf. Equation B.4) with $\mathbf{M} = \mathbf{D}_{\mathbf{r}}^{-1}$ and $\mathbf{W} = \mathbf{D}_{\mathbf{c}}^{-1}$. As a result, this maximization can be solved by the alternating least squares (ALS) Algorithm (see Algorithm E.2 in Appendix F.

In CA, each column of $\mathbf{U}$ (respectively $\mathbf{V}$) stores the loadings for rows (respectively columns) to compute the row

factor scores (denoted $\mathbf{F}$) and the column factor scores (denoted $\mathbf{G}$) of each component, where

$$\mathbf{F} = \mathbf{D}_\mathbf{r}^{-1}\mathbf{U}\boldsymbol{\Delta} = \mathbf{D}_\mathbf{r}^{-1}\mathbf{X}\mathbf{D}_\mathbf{c}^{-1}\mathbf{V} \quad \text{and} \quad \mathbf{G} = \mathbf{D}_\mathbf{c}^{-1}\mathbf{V}\boldsymbol{\Delta} = \mathbf{D}_\mathbf{c}^{-1}\mathbf{X}^\top\mathbf{D}_\mathbf{r}^{-1}\mathbf{U}. \tag{5}$$

For each component, the contributions of the rows and the columns are computed from the squared weighted loadings:

$$\mathbf{ctr}_{\mathbf{r},\ell} = \left(\mathbf{D}_\mathbf{r}^{-\frac{1}{2}}\mathbf{u}_\ell\right) \odot \left(\mathbf{D}_\mathbf{r}^{-\frac{1}{2}}\mathbf{u}_\ell\right) \quad \text{and} \quad \mathbf{ctr}_{\mathbf{c},\ell} = \left(\mathbf{D}_\mathbf{c}^{-\frac{1}{2}}\mathbf{v}_\ell\right) \odot \left(\mathbf{D}_\mathbf{c}^{-\frac{1}{2}}\mathbf{v}_\ell\right), \tag{6}$$

where the contributions of a given component sum to 1 (i.e., $\mathbf{u}_\ell^\top\mathbf{D}_\mathbf{r}^{-1}\mathbf{u}_\ell = \mathbf{v}_\ell^\top\mathbf{D}_\mathbf{c}^{-1}\mathbf{v}_\ell = 1$).

For sCA, gsGSVD is used to sparsify the generalized singular vectors and gives generalized *pseudo*-singular vectors with sparsified loadings shrunken to 0 to facilitate the interpretation of components. The sparsification of CA is a specific case of the gsGSVD where the row metric matrix $\mathbf{M}$ equals $\mathbf{D}_\mathbf{r}^{-1}$ and the column metric matrix $\mathbf{W}$ equals $\mathbf{D}_\mathbf{c}^{-1}$. When the data include group structures for rows or columns and should, therefore, be sparsified accordingly, the group constraints can be applied by specifying the sparsification parameters $s_{\mathbf{p},\ell}$ and $s_{\mathbf{q},\ell}$ to include group designs of rows and of columns. When group constraints are not included, the algorithm becomes the sGSVD (Algorithm E.4 in Appendix F).

In the sCA algorithm, the POCS procedure projects the data onto the intersection of three constrained spaces: 1) the $\mathcal{L}_2$-ball that normalizes the singular vectors, 2) the orthogonal space (i.e., $\mathbf{P}_\ell^\perp$ or $\mathbf{Q}_\ell^\perp$) that ensures orthogonality between components, and 3) the $\mathcal{L}_1$-ball that sparsifies the elements of the (generalized) singular vectors (i.e., $\mathbf{p}$, $\mathbf{q}$, $\mathbf{u}$, and $\mathbf{v}$) or the $\mathcal{L}_\mathcal{G}$-ball if they are sparsified in groups.

From the generalized pseudo-singular vectors, the factor scores are computed as:

$$\mathbf{F} = \mathbf{D}_\mathbf{r}^{-1}\mathbf{U}\boldsymbol{\Delta} \quad \text{and} \quad \mathbf{G} = \mathbf{D}_\mathbf{c}^{-1}\mathbf{V}\boldsymbol{\Delta}. \tag{7}$$

It is worth noting that, with sparsification,

$$\mathbf{F} \neq \mathbf{D}_\mathbf{r}^{-1}\mathbf{X}\mathbf{D}_\mathbf{c}^{-1}\mathbf{V} \quad \text{and} \quad \mathbf{G} \neq \mathbf{D}_\mathbf{c}^{-1}\mathbf{X}^\top\mathbf{D}_\mathbf{r}^{-1}\mathbf{U}. \tag{8}$$

The loss of these properties is discussed in Section 3.3. Here, we choose to compute the factor scores as the scaled generalized pseudo-singular vectors (i.e., Equation 7) over the linear combinations of the original data (i.e., Equation 8) so that the sparsity of the generalized pseudo-singular vectors propagates to the factor scores.

3.2.2. Discriminant simple CA (DiSCA) and sDiSCA: sparsification for discriminant analysis

The discriminant analysis of simple CA (as opposed to *multiple* CA) is used to analyze a contingency table with rows nested in groups when we aim to extract components that best explain the inertia *between* these groups of rows. To do so, DiSCA performs CA on the group sums across the rows. Formally, DiSCA computes the matrix of group sums (denoted by $\mathbf{A}_\mathcal{G}$) with an $I \times I_\mathcal{G}$ indicator matrix $\mathbf{H}$ with 1s (and 0s otherwise) indicating the group belonging

of the rows. $\mathbf{A}_{\mathcal{G}}$ is therefore computed as:

$$\mathbf{A}_{\mathcal{G}} = \mathbf{H}^{\top}\mathbf{A}, \tag{9}$$

where the rows of $\mathbf{A}_{\mathcal{G}}$ correspond to $I_{\mathcal{G}}$ row groups and the columns of $\mathbf{A}_{\mathcal{G}}$ correspond to the J levels of the categorical variable on the columns. Similar to CA, DiSCA then computes the probability matrix by dividing $\mathbf{A}_{\mathcal{G}}$ by its total N:

$$\mathbf{Z}_{\mathcal{G}} = \frac{1}{N}\,\mathbf{A}_{\mathcal{G}}. \tag{10}$$

Next, this probability matrix $\mathbf{Z}_{\mathcal{G}}$ is double centered with Equation 3 to give the resulting matrix $\mathbf{X}_{\mathcal{G}}$, which is then decomposed by the GSVD with Equation 4. Then, we define $\mathbf{D}_{\mathbf{r},\mathcal{G}}^{-1}$ as the row metric matrix of $\mathbf{X}_{\mathcal{G}}$. Finally, the row and column factors are computed the same way as in CA:

$$\mathbf{F} = \mathbf{D}_{\mathbf{r},\mathcal{G}}^{-1}\mathbf{U}\boldsymbol{\Delta} = \mathbf{D}_{\mathbf{r},\mathcal{G}}^{-1}\mathbf{X}_{\mathcal{G}}\mathbf{D}_{\mathbf{c}}^{-1}\mathbf{V} \quad \text{and} \quad \mathbf{G} = \mathbf{D}_{\mathbf{c}}^{-1}\mathbf{V}\boldsymbol{\Delta} = \mathbf{D}_{\mathbf{c}}^{-1}\mathbf{X}_{\mathcal{G}}^{\top}\mathbf{D}_{\mathbf{r},\mathcal{G}}^{-1}\mathbf{U}. \tag{11}$$

The contributions of rows and columns can also be computed from the generalized singular vectors with Equation 6.

In DiSCA, the row factor score $f_{i,\ell}$ represents the $i_{\mathcal{G}}$th group on the ℓth component, and the column factor scores $g_{j,\ell}$ represents the jth column on the ℓth component. The individuals within each group, which are stored in rows of $\mathbf{A}$, can be projected onto the component space as supplementary rows. Formally, if the ith row, denoted $\mathbf{a}_i^{\top}$, is projected onto the components as $\mathbf{f}_i^*$, then

$$\mathbf{f}_i^* = \left(\mathbf{a}_i^{\top}\mathbf{1}\right)^{-1}\boldsymbol{\Delta}^{-1}\mathbf{G}^{\top}\mathbf{a}_i. \tag{12}$$

To sparsify DiSCA, sDiSCA uses the gsGSVD to sparsify the generalized singular vectors and computes the generalized *pseudo*-singular vectors. Just like sCA, sDiSCA is a specific case of the gsGSVD where the row metric matrix $\mathbf{M}$ equals $\mathbf{D}_{\mathbf{r},\mathcal{G}}^{-1}$ and the column metric matrix $\mathbf{W}$ equals $\mathbf{D}_{\mathbf{c}}^{-1}$ with optional group constraints that can be implemented by specifying the sparsification parameters $s_{\mathbf{p},\ell}$ and $s_{\mathbf{q},\ell}$. The only difference is that the row metrics are now computed from the row groups instead of from the individual rows. From these generalized pseudo-singular vectors, the factor scores are computed in the same way as in sCA using Equation 7.

Just like in sCA, the POCS procedure in the algorithm of sDiSCA projects the data onto the intersection of three constrained spaces: 1) the $\mathcal{L}_2$-ball that normalizes the singular vectors, 2) the orthogonal space (i.e., $\mathbf{P}_{\ell}^{\perp}$ or $\mathbf{Q}_{\ell}^{\perp}$) that ensures orthogonality between components, and 3) the $\mathcal{L}_1$-ball that sparsifies the elements of the (generalized) singular vectors (i.e., $\mathbf{p}$, $\mathbf{q}$, $\mathbf{u}$, and $\mathbf{v}$) or the $\mathcal{L}_{\mathcal{G}}$-ball if they are sparsified in groups.

3.2.3. MCA and sparse MCA (sMCA): sparsification with metric matrices and group constraints for columns

MCA extends CA to analyze the association between more than two categorical variables by using an *indicator matrix* to represent each variable with a group of 0/1 columns (Greenacre, 1984; Lebart et al., 1984; Abdi and Valentin, 2007). where each columns codes a level of this variable with a value of 1 indicating this level. MCA concatenates the

indicator matrices of all variables and then uses CA to extract orthogonal components from this concatenated table.

Formally, consider a matrix $\mathbf{A}$ with I observations and K categorical variables. where J_k denotes the number of levels of the kth variable and with a total of $J = \sum_{k=1}^{K} J_k$ columns. Matrix $\mathbf{A}$ with a sub-table structure of indicator matrices can be expressed as

$$\mathbf{A} = [\mathbf{A}_1 \mid \mathbf{A}_2 \mid \mathbf{A}_3 \mid \cdots \mid \mathbf{A}_k \mid \cdots \mid \mathbf{A}_K], \tag{13}$$

where $\mathbf{A}_k$ is the indicator matrix for the kth categorical variable. Note that the sum of each row of $\mathbf{A}$ equals K and the total sum of each $\mathbf{A}_k$ equals I. Just like in CA, MCA first computes the probability matrix $\mathbf{Z}$ by dividing $\mathbf{A}$ by the sum of all it entries (cf. Equation 2):

$$\mathbf{Z} = \frac{1}{IK}\mathbf{A}, \tag{14}$$

and then double centers the probability matrix by (cf. Equation 3):

$$\mathbf{X} = \mathbf{Z} - \mathbf{r}\mathbf{c}^\top, \tag{15}$$

where $\mathbf{r}$ is a vector that stores the sums of each row (i.e., $\mathbf{r} = \mathbf{Z}\mathbf{1}$) and $\mathbf{c}$ is a vector that stores the sums of each column (i.e., $\mathbf{c} = \mathbf{Z}^\top\mathbf{1}$). This double centered probability matrix $\mathbf{X}$ is then analyzed by the GSVD:

$$\mathbf{X} = \mathbf{U}\boldsymbol{\Delta}\mathbf{V}^\top \quad \text{subject to} \quad \mathbf{U}^\top\mathbf{D}_\mathbf{r}^{-1}\mathbf{U} = \mathbf{V}^\top\mathbf{D}_\mathbf{c}^{-1}\mathbf{V} = \mathbf{I}, \tag{16}$$

where $\mathbf{D}_\mathbf{r} = \mathsf{diag}(\mathbf{r})$, $\mathbf{D}_\mathbf{c} = \mathsf{diag}(\mathbf{c})$, and $\boldsymbol{\Delta}$ is the diagonal matrix storing the generalized eigenvalues. In addition, just like in CA, such a GSVD is equivalent to the SVD from Equation B.5 and solves the same maximization problem (cf. Equation B.4) with $\mathbf{M} = \mathbf{D}_\mathbf{r}^{-1}$ and $\mathbf{W} = \mathbf{D}_\mathbf{c}^{-1}$. As a result, this maximization can be solved by the same Algorithm E.2 as for CA. Finally, the row and column factors are computed as in CA:

$$\mathbf{F} = \mathbf{D}_\mathbf{r}^{-1}\mathbf{U}\boldsymbol{\Delta} = \mathbf{D}_\mathbf{r}^{-1}\mathbf{X}\mathbf{D}_\mathbf{c}^{-1}\mathbf{V} \quad \text{and} \quad \mathbf{G} = \mathbf{D}_\mathbf{c}^{-1}\mathbf{V}\boldsymbol{\Delta} = \mathbf{D}_\mathbf{c}^{-1}\mathbf{X}^\top\mathbf{D}_\mathbf{r}^{-1}\mathbf{U}. \tag{17}$$

In MCA, the row factor scores $\mathbf{f}_{i,\ell}$ represents the ith observation on the ℓth component, and the column factor scores $\mathbf{g}_{j_k,\ell}$ represent the jth level of the kth variable on the ℓth component.

To sparsify MCA, we sparsify the left and right generalized singular vectors of MCA and derive *generalized pseudo-singular vectors* where the sparse loadings are shrunken to 0. The sparsification of MCA is a specific case of the gsGSVD (Algorithm 1), similar to sCA, with the row metric matrix $\mathbf{D}_\mathbf{r}^{-1}$, the column metric matrix $\mathbf{D}_\mathbf{c}^{-1}$, and a (*non-optional*) group constraint $\mathcal{G}_\mathbf{q}$ on the columns. This group constraint ensures that when the kth variable is kept or sparsified, all the J_k columns associated with its levels kept or sparsified together. Such group sparsification can be optionally imposed on the rows (i.e., the observations) by specifying $\mathcal{G}_\mathbf{p}$ when the rows are expected to be kept or dropped according to their groups.

In the gsGSVD algorithm used for sMCA, the POCS procedure projects the data onto the intersection of three

constrained spaces: 1) the $\mathcal{L}_2$-ball that normalizes the singular vectors, 2) the orthogonal space (i.e., $\mathbf{P}_\ell^\perp$ or $\mathbf{Q}_\ell^\perp$) that ensures orthogonality, and 3) the $\mathcal{L}_\mathcal{G}$-ball that sparsifies the elements of the right, and sometimes also the left, singular vectors (i.e., $\mathbf{p}$ and $\mathbf{q}$) and generalized singular vectors (i.e., $\mathbf{u}$ and $\mathbf{v}$) in groups.

3.2.4. Discriminant MCA (DiMCA) and sDiMCA: sparsification for discriminant analysis with group constraints for columns

The discriminant version of MCA (DiMCA) analyzes a matrix with variables codeed as for MCA with rows nested in groups and extracts components that best explain the inertia *between groups*. To do so, DiMCA performs MCA on the group sums across the rows of the concatenated table.

Formally, consider the same $I \times J$ data set $\mathbf{A}$ as used for MCA (see Equation 13), if the observation groups are represented by an $I \times I_\mathcal{G}$ indicator matrix $\mathbf{H}$, the matrix of group sums across the observations (denoted by $\mathbf{A}_\mathcal{G}$) is computed as:

$$\mathbf{A}_\mathcal{G} = \mathbf{H}^\top \mathbf{A}, \tag{18}$$

where the rows of $\mathbf{A}_\mathcal{G}$ correspond to the $I_\mathcal{G}$ observation groups and the columns of $\mathbf{A}_\mathcal{G}$ correspond to the levels of all K categorical variables (i.e., $J = \sum_1^K J_k$). Just like in MCA, the double centered probability matrix $\mathbf{X}_\mathcal{G}$ is obtained from the probability matrix $\mathbf{Z}_\mathcal{G}$ as (cf. Equations 14 and 15):

$$\mathbf{Z}_\mathcal{G} = \frac{1}{IK}\,\mathbf{A}_\mathcal{G} \quad \text{and} \quad \mathbf{X}_\mathcal{G} = \mathbf{Z}_\mathcal{G} - \mathbf{r}\mathbf{c}^\top, \tag{19}$$

where $\mathbf{r}$ is a vector that stores the row sums (i.e., $\mathbf{r} = \mathbf{Z}_\mathcal{G}\mathbf{1}$) and $\mathbf{c}$ is a vector that stores column sums (i.e., $\mathbf{c} = \mathbf{Z}_\mathcal{G}^\top\mathbf{1}$). $\mathbf{X}_\mathcal{G}$ is then analyzed by the GSVD:

$$\mathbf{X}_\mathcal{G} = \mathbf{U}\boldsymbol{\Delta}\mathbf{V}^\top \quad \text{subject to} \quad \mathbf{U}^\top\mathbf{D}_{\mathbf{r},\mathcal{G}}^{-1}\mathbf{U} = \mathbf{V}^\top\mathbf{D}_\mathbf{c}^{-1}\mathbf{V} = \mathbf{I}, \tag{20}$$

where $\mathbf{D}_{\mathbf{r},\mathcal{G}} = \mathsf{diag}\,(\mathbf{r})$, $\mathbf{D}_\mathbf{c} = \mathsf{diag}\,(\mathbf{c})$, and $\boldsymbol{\Delta}$ is the diagonal matrix of the generalized eigenvalues. In addition, just like in CA and MCA, this GSVD is equivalent to the SVD of Equation B.5 and solves the same maximization problem (cf. Equation B.4) with $\mathbf{M} = \mathbf{D}_{\mathbf{r},\mathcal{G}}^{-1}$ and $\mathbf{W} = \mathbf{D}_\mathbf{c}^{-1}$. As a result, this maximization can also be solved by Algorithm E.2. Finally, the row and column factors are computed as for CA and MCA:

$$\mathbf{F} = \mathbf{D}_{\mathbf{r},\mathcal{G}}^{-1}\mathbf{U}\boldsymbol{\Delta} = \mathbf{D}_{\mathbf{r},\mathcal{G}}^{-1}\mathbf{X}\mathbf{D}_\mathbf{c}^{-1}\mathbf{V} \quad \text{and} \quad \mathbf{G} = \mathbf{D}_\mathbf{c}^{-1}\mathbf{V}\boldsymbol{\Delta} = \mathbf{D}_\mathbf{c}^{-1}\mathbf{X}^\top\mathbf{D}_{\mathbf{r},\mathcal{G}}^{-1}\mathbf{U}. \tag{21}$$

In DiMCA, the row factor scores $\mathbf{f}_{i,\ell}$ represent the $i_\mathcal{G}$th observation group on the ℓth component, and the column factor scores $\mathbf{g}_{j_k,\ell}$ represent the jth level of the kth variable on the ℓth component.

Finally, the original observations can be projected onto the component space as supplementary elements. Formally,

the ith observation denoted by $\mathbf{a}_i$ (i.e., the ith row of $\mathbf{A}$) is projected onto the components to obtain $\mathbf{f}_i^*$ computed as

$$\mathbf{f}_i^* = \left(\mathbf{a}_i^\top \mathbf{1}\right)^{-1} \mathbf{a}_i^\top \mathbf{G}\boldsymbol{\Delta}^{-1}. \tag{22}$$

To sparsify DiMCA, we sparsify the left and right generalized singular vectors of DiMCA and derive *generalized pseudo-singular vectors* where the sparse loadings are shrunken to 0. Just like the other sparse methods, sDiMCA is a specific case of the gsGSVD (Algorithm 1) with row metric matrix $\mathbf{D}_{\mathbf{r},\mathcal{G}}^{-1}$, column metric matrix $\mathbf{D}_{\mathbf{c}}^{-1}$, and the group constraint $\mathcal{G}_{\mathbf{q}}$ (on the columns). Here, the POCS procedure works the same as in sMCA.

3.3. Sparsification: Lost and found properties

Because of its specific preprocessing steps and metric constraints, CA (and therefore MCA, DiSCA, and DiMCA) possesses six essential properties: transition formulas, supplementary projections, asymmetric projection, distributional equivalence, barycentric projection, and embedded solutions (see Lebart et al., 1984, and Appendix C for details). As sparsification introduces non-differentiable constraints into the optimization problem, the projection operators used for obtaining sparse solutions are non-linear. This non-linearity leads to a situation where the properties, which predominantly depend on linearity in standard CA-related methods, are either partially retained with minor modifications or completely lost. In this section, we identify these lost properties and evaluate possible solutions to restore them.

Property 3.1. *Transition formulas: from rows to columns and back*

The transition formulas allow row factor scores ($\mathbf{f}_\ell$) to be derived from the column factor scores ($\mathbf{g}_\ell$), and vice versa (see, Escofier 1979, the original transition formulas are also described in Property C.1). However, the original transition formulas no longer work with the gsGSVD because these formulas are linear projections whereas the projecting operator in Algorithm 1 is not linear. With such a non-linear projecting operator, we developed new transition formulas (with slight modifications from the original ones) that integrate the same non-linear projection as follows:

$$\begin{aligned}
\mathbf{f}_\ell &= \mathbf{D}_{\mathbf{r}}^{-1}\mathbf{u}_\ell\delta_\ell \\
&= \mathbf{D}_{\mathbf{r}}^{-1} \cdot \mathbf{D}_{\mathbf{r}}^{\frac{1}{2}} \operatorname{proj}_{\mathcal{L}_{\mathcal{G}_{\mathbf{u}}}\cap\mathcal{L}_2\cap\mathbf{P}^\perp}\left(\mathbf{D}_{\mathbf{r}}^{-\frac{1}{2}}\mathbf{X}\mathbf{D}_{\mathbf{c}}^{-1}\mathbf{v}_\ell\right)\delta_\ell \\
&= \mathbf{D}_{\mathbf{r}}^{-\frac{1}{2}} \operatorname{proj}_{\mathcal{L}_{\mathcal{G}_{\mathbf{u}}}\cap\mathcal{L}_2\cap\mathbf{P}^\perp}\left(\mathbf{D}_{\mathbf{r}}^{-\frac{1}{2}}\mathbf{X}\mathbf{D}_{\mathbf{c}}^{-1}\mathbf{v}_\ell\right)\delta_\ell,
\end{aligned} \tag{23}$$

$$\begin{aligned}
\mathbf{g}_\ell &= \mathbf{D}_{\mathbf{c}}^{-1}\mathbf{v}_\ell\delta_\ell \\
&= \mathbf{D}_{\mathbf{c}}^{-1} \cdot \mathbf{D}_{\mathbf{c}}^{\frac{1}{2}} \operatorname{proj}_{\mathcal{L}_{\mathcal{G}_{\mathbf{v}}}\cap\mathcal{L}_2\cap\mathbf{Q}^\perp}\left(\mathbf{D}_{\mathbf{c}}^{-\frac{1}{2}}\mathbf{X}^\top\mathbf{D}_{\mathbf{r}}^{-1}\mathbf{u}_\ell\right)\delta_\ell \\
&= \mathbf{D}_{\mathbf{c}}^{-\frac{1}{2}} \operatorname{proj}_{\mathcal{L}_{\mathcal{G}_{\mathbf{v}}}\cap\mathcal{L}_2\cap\mathbf{Q}^\perp}\left(\mathbf{D}_{\mathbf{c}}^{-\frac{1}{2}}\mathbf{X}^\top\mathbf{D}_{\mathbf{r}}^{-1}\mathbf{u}_\ell\right)\delta_\ell.
\end{aligned} \tag{24}$$

When $\ell = 1$, $\mathbf{P}^\perp = \mathbf{Q}^\perp = \mathbf{0}$, and when $\ell > 1$, $\mathbf{P}^\perp = \left[\mathbf{p}_1 \mid \cdots \mid \mathbf{p}_{\ell-1}\right]$ and $\mathbf{Q}^\perp = \left[\mathbf{q}_1 \mid \cdots \mid \mathbf{q}_{\ell-1}\right]$.

These transition formulas for the gsGSVD are valid when (1) all the constraints are satisfied, and (2) the estimated pseudo-singular vectors $\mathbf{P}$ and $\mathbf{Q}$ are in the order in which they were estimated by the ALS algorithm. Specifically, in our algorithm, the number of dimensions is specified, and the dimensions are reordered after all requested ones are estimated to give the pseudo-singular values in descending order . This reordering step is necessary because there is no theoretical guarantee that Algorithm 1 estimates pseudo-singular values in a descending order. Remark (2) is especially important, because this order influences the definition of $\mathbf{P}^{\perp}$ and $\mathbf{Q}^{\perp}$ for a given ℓ. As a result, the number of dimensions is one of the hyperparameters that can also lead to different results and should be evaluated and optimized (see Section 3.4 for details).

Property 3.2. *Supplementary projections.*

In CA/MCA/DiSCA/DiMCA, rows and columns can be projected as *supplementary elements* using equations from Property C.2. Even though the equations for supplementary projection are directly derived from the transition formulas, the projection of supplementary elements no longer works as in the regular versions of CA-related methods. The new transition formulas are defined in Equations 23 and 24. When applied to a subset of existing rows or columns of $\mathbf{X}$, the transition formulas are not guaranteed to recover the correct sparse factor scores given by the full sparse decomposition of $\mathbf{X}$; When applied to new data, we observed that the transition formulas could give incoherent results; specifically new data numerically close to existing data could be projected very far away from each other. This problem occurs because the non-linear projector requires the full set of data (i.e., the data matrix $\mathbf{X}$).Because $\mathbf{X}$ is not fully decomposed with sparsification, there might not exist $\mathbf{u}_R$ and $\mathbf{v}_R$ for all R dimensions to perfectly reconstruct $\mathbf{X}$.

To mitigate this issue, we define a rank-R approximation of $\mathbf{X}$ by $\widehat{\mathbf{X}}$:

$$\widehat{\mathbf{X}} = \mathbf{U}\widehat{\mathbf{\Delta}}\mathbf{V}^{\top}, \tag{25}$$

where $\mathbf{U}$, $\widehat{\mathbf{\Delta}}$, $\mathbf{V}$ are given by Equation 1. Based on $\widehat{\mathbf{X}}$, we compute two projector matrices for the transition formula: 1) one projects $\mathbf{X}$ onto the space of $\widehat{\mathbf{X}}$ (denoted by $\mathbf{\Omega_r}$) and 2) the other one projects $\mathbf{X}^{\top}$ onto the space of $\widehat{\mathbf{X}}^{\top}$ (denoted by $\mathbf{\Omega_c}$). These linear projector matrices thus approximate the non-linear projectors and are obtained as:

$$\begin{aligned} \mathbf{\Omega_r} &= (\mathbf{X}\mathbf{X}^{\top})^{-1}\mathbf{X}(\widehat{\mathbf{X}}^{\top}), \\ \mathbf{\Omega_c} &= (\mathbf{X}^{\top}\mathbf{X})^{-1}\mathbf{X}^{\top}(\widehat{\mathbf{X}}), \end{aligned} \tag{26}$$

which is equivalent to using a pseudo-inverse as a projector.

Formally, the factor score of a supplementary row $\mathbf{i}_{\text{sup}}$ (denoted $\mathbf{f}^{*}_{\text{sup}}$) is computed from Equation 23 as:

$$\mathbf{f}^{*}_{\text{sup}} = \left(\mathbf{i}^{\top}_{\text{sup}}\mathbf{1}\right)^{-1}\mathbf{i}^{\top}_{\text{sup}}\mathbf{\Omega_c}\mathbf{G}\mathbf{\Delta}^{-1}. \tag{27}$$

The factor score of a supplementary column $\mathbf{j}_{\text{sup}}$ (denoted $\mathbf{g}^*_{\text{sup}}$) is computed from Equation 24 as:

$$\mathbf{g}^*_{\text{sup}} = \left(\mathbf{1}^\top \mathbf{j}_{\text{sup}}\right)^{-1} \mathbf{j}_{\text{sup}}^\top \boldsymbol{\Omega}_{\mathbf{r}} \mathbf{F} \boldsymbol{\Delta}^{-1}. \tag{28}$$

However, when there is no linear transformation from the data in $\mathbf{X}$ to the component space of $\widehat{\mathbf{X}}$, these new formulas for supplementary projections will provide only an approximation.

Property 3.3. *The asymmetric projection.*

The asymmetric projections of rows or columns give factor scores with unitary inertia (Property C.6). With sparsification, the asymmetric projections can be derived from the new transition formulas and are computed differently from Equations C.11 and C.13. The asymmetric projections of the rows $\widetilde{\mathbf{F}}^*_\ell$ are computed as:

$$\widetilde{\mathbf{F}}^* = \mathbf{D}_{\mathbf{r}}^{-1}\mathbf{U} \quad \text{with its inertia} \quad \widetilde{\mathbf{F}}^{*\top}\mathbf{D}_{\mathbf{r}}\widetilde{\mathbf{F}}^* = \mathbf{I}. \tag{29}$$

Similarly, the asymmetric projections of the columns $\widetilde{\mathbf{G}}^*_\ell$ are computed as:

$$\widetilde{\mathbf{G}}^* = \mathbf{D}_{\mathbf{c}}^{-1}\mathbf{V} \quad \text{with its inertia} \quad \widetilde{\mathbf{G}}^{*\top}\mathbf{D}_{\mathbf{c}}\widetilde{\mathbf{G}}^* = \mathbf{I}. \tag{30}$$

These asymmetric projections of CA/MCA/DiSCA/DiMCA are preserved in the gsGSVD with sparsification.

Property 3.4. *Distributional equivalence: Rows (or columns) proportional to each other can be replaced by their sum without affecting the results of the analysis.*

Because these methods analyze the frequencies of the occurrences, two rows (or two columns) proportional to each other have identical profiles (i.e., see Escofier, 1969, for details.) Therefore these rows (or columns) are represented by *two* points having the same coordinates in the component space, and so these two points can be merged into *one* whose mass is the sum of their original masses (Escofier, 1969; Fichet, 2009; Benzécri et al., 1973; Greenacre, 1984). In addition, merging these two points does not change the geometry of the component space. This property is kept in gsGSVD with sparsification.

Property 3.5. *Barycentric projection: the barycenters of the row factor scores, and the column factor scores are equal to the null vector (Escofier, 1969).*

The row and the column factor scores of CA/MCA/DiSCA/DiMCA share a common barycenter (i.e., weighted mean) of 0; Formally

$$\frac{1}{I}\mathbf{r}^\top \mathbf{f}_\ell = \frac{1}{J}\mathbf{c}^\top \mathbf{g}_\ell = 0. \tag{31}$$

Specifically in MCA and DiMCA, the barycenter of each variable (i.e., set of columns) is null:

$$\sum_{j=1}^{J_k} c_{j,k}\mathbf{g}_{j,k,\ell} = 0, \tag{32}$$

where $c_{j,k}$ is the column weight for the jth level of the kth variable, and $\mathbf{g}_{j,k,\ell}$ is the factor scores of the jth level of the kth variable on the ℓth component. In addition, all observations that belong to a given variable level, have their mean row factor scores equal to the column factor score of this variable level. This property is lost in sCA and sDiSCA because the $\text{proj}_{\mathcal{L}_1}$ operator sparsifies the variable levels individually on rows and/or columns. However, this property is kept in sMCA and sDiMCA, because these methods use internally the $\text{proj}_{\mathcal{L}_\mathcal{G}}$ operator to keep or sparsify the levels of each variable in groups, which conserves their barycenters. Simulation results are illustrated in *** Figure XX.***

Property 3.6. *Embedded solution: The GSVD of the non-centered matrix (i.e.,* $\mathbf{Z}$*) has a first singular value of 1, a first left generalized singular vector equal to* $\mathbf{r}$*, and a first right generalized singular vector equal to* $\mathbf{c}$*. In addition, the subsequent components are the same as those of the GSVD of the double centered matrix* $\mathbf{X}$*.*

The embedded solution holds because the GSVD in CA (Equation 4) can be rewritten as:

$$\begin{aligned} \mathbf{X} = \mathbf{Z} - \mathbf{r}\mathbf{c}^\top = \mathbf{U}\boldsymbol{\Delta}\mathbf{V}^\top = \sum_{\ell=1}^{L} \delta_\ell \mathbf{u}_\ell \mathbf{v}_\ell^\top \\ \text{under the constraints} \quad \mathbf{U}^\top \mathbf{D}_\mathbf{r}^{-1}\mathbf{U} = \mathbf{V}^\top \mathbf{D}_\mathbf{c}^{-1}\mathbf{V} = \mathbf{I} \end{aligned} \tag{33}$$

which gives

$$\begin{aligned} \mathbf{Z} = \mathbf{r}\mathbf{c}^\top + \mathbf{U}\boldsymbol{\Delta}\mathbf{V}^\top = 1 \times \mathbf{r}\mathbf{c}^\top + \sum_{\ell=2}^{L} \delta_\ell \mathbf{u}_\ell \mathbf{v}_\ell^\top \\ \text{under the constraints} \quad \mathbf{U}^\top \mathbf{D}_\mathbf{r}^{-1}\mathbf{U} = \mathbf{V}^\top \mathbf{D}_\mathbf{c}^{-1}\mathbf{V} = \mathbf{I}. \end{aligned} \tag{34}$$

Therefore, when the non-centered data $\mathbf{Z}$ is analyzed, the first generalized singular value δ_1 equals 1, the first left generalized singular vector $\mathbf{u}_1$ equals $\mathbf{r}$, and the first right generalized singular vector $\mathbf{v}_1$ equals $\mathbf{c}$. With $\mathbf{r}\mathbf{c}^\top$ computing the *expected* frequencies of $\mathbf{Z}$ under independence, the CA of $\mathbf{X}$, where $\mathbf{X} = \mathbf{Z} - \mathbf{r}\mathbf{c}^\top$, analyzes the deviation of the *observed* data (i.e., $\mathbf{Z}$) from independence (i.e., as given by matrix $\mathbf{r}\mathbf{c}^\top$).

When the singular vectors are sparsified, the embedded solution of the CA/MCA/DiSCA/DiMCA (Property C.5) framework does not hold. Therefore, when the non-centered data $\mathbf{Z}$ is analyzed by sCA/sMCA/sDiSCA/sDiMCA, the first pseudo-singular-value δ_1 will be close to, but smaller than, 1, the first left (respectively right) generalized pseudo-singular-vector $\mathbf{u}_1$ (respectively $\mathbf{v}_1$) will be close to but not equal to $\mathbf{r}$ (respectively $\mathbf{c}$).

3.4. Evaluating the sparsification

The most straightforward way to evaluate the sparsity of left and right pseudo-generalized singular vectors is to express their number of zeros as a function of s (i.t., the sparsity parameter). Liu et al. (2023) noted that such a crude index of sparsity would not be useful for choosing an "optimal" value for the sparsity parameters. Recently, Trendafilov et al.'s (2017) sparsity index combines two measures: a measure of sparsity and a measure of how close the reduced rank sparse matrix is to the original data matrix.

We measure sparsity with three different indices: 1) $\vartheta_{\mathbf{P}}$, the ratio of the number of zeros to the total number of coefficients in the loading matrix $\mathbf{P}$, and 2) its counterpart $\vartheta_{\mathbf{Q}}$, the ratio of the number of zeros to the total number of coefficients in the loading matrix $\mathbf{Q}$, and 3) ϑ, the ratio of the number of zeros in both $\mathbf{P}$ and $\mathbf{Q}$ to the total number of coefficients in $\mathbf{P}$ and $\mathbf{Q}$.

$$\begin{aligned}
\vartheta_{\mathbf{P}} &= \frac{\#_0(\mathbf{P})}{I \times \ell} \\
\vartheta_{\mathbf{Q}} &= \frac{\#_0(\mathbf{Q})}{J \times \ell} \\
\vartheta &= \frac{\#_0(\mathbf{P}) + \#_0(\mathbf{Q})}{(I+J) \times \ell}
\end{aligned} \tag{35}$$

Given L being the specified number of dimensions to estimate, we measure the fit, noted $\hat{\tau}$, as the ratio of the sum of the L squared pseudo-singular values to the sum of the first L squared singular values:

$$\hat{\tau} = \frac{\sum_{\ell=1}^{L} \hat{\delta}_\ell^2}{\sum_{\ell=1}^{L} \delta_\ell^2} \tag{36}$$

Combining both two types of ratios (sparsity and fit), gives three different sparsity indices:

$$\begin{aligned}
\varsigma_{\mathbf{P}} &= \vartheta_{\mathbf{P}} \times \hat{\tau} \\
\varsigma_{\mathbf{Q}} &= \vartheta_{\mathbf{Q}} \times \hat{\tau} \\
\varsigma &= \vartheta \times \hat{\tau},
\end{aligned} \tag{37}$$

where $\varsigma_{\mathbf{P}}$ is the compromise between fit and sparsity for the left generalized singular vectors, $\varsigma_{\mathbf{Q}}$ is the compromise between fit and sparsity for the right generalized singular vectors, and ς is the compromise between fit and sparsity for both the left and the right generalized singular vectors.

Depending on the application, the analyst can use one or more of these three sparsity indices to select the appropriate value of the sparsity parameters $s_{\mathbf{p}}$ and $s_{\mathbf{q}}$. We illustrate these indices in the result section.

Figure 1 depicts the range of possible values for the sparsity indices on a graph representing the ratio of zeros on the x-axis and the "fit" on the y-axis. On this figure, the result of a sparse analysis would be represented as a dot, according to how sparse the loadings are ("zero ratio") and how close the lower rank sparse decomposition of the data is to the original data ("fit"). We split the graph into 5 zones: Zones 1 to 3 correspond to a low sparsity index because either or both "fit" and "zero ratio" are close to zero, Zone 4 corresponds to a sparsity index close to its maximum value of 1, when very few variables are selected and they represent most of the information in the data, and, finally, Zone 5 corresponds to a middle ground, where a compromise is reached between sparsity and fit. In the following Result section, we will provide such map for each example. The optimal value for the sparsity parameters and the number of dimensions will be chosen by maximizing the sparsity index.

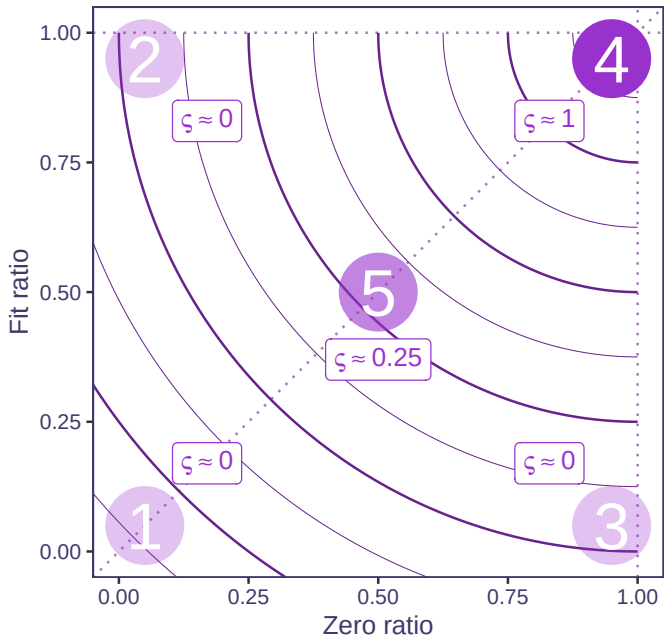

Figure 1. Graph representing different possible values for the sparsity index on a map of the "fit" as a function of the "zero ratio." The five zones represent five possible combinations of the two ratios, along with the corresponding values of the sparsity index ς.

4. Results

4.1. sCA

4.1.1. Data

We applied sparse Correspondence Analysis to a contingency table storing the number of deaths in the USA in 2018 as a function of age and causes of death. The causes of death were categorized according to the International Statistical Classification of Diseases and Related Health Problems (ICD) (World Health Organization, 2019). We

grouped the ages of death by every 5 years starting from the age of 1 and summing all deaths above 100 years old into a single group called "100+." In addition, we removed the deaths before the age of 1 because they mostly belong to a single category of the perinatal causes. Including this age group would lead to this specific cause-age association dominating the result and shadowing other effects as deaths resulting from perinatal causes were rare in other age groups (i.e., 57 out of 118 cases were before 1 year old with the other 61 cases spread across the other 21 age groups.). The resulting data analyzed by CA and sCA was a 21 (age groups) by 19 (causes of death) contingency table with counts indicating the number of deaths of each cause at each age range.

4.1.2. Results

Figure 2A shows the scree plot of the sCA result. Here, we only consider solutions with more than 2 components and found that sCA with 2 components gave the optimal result, which has the sparsest solution with the largest fit. These characteristics are indicated in Figure 2B, which illustrates the sparsity index of possible solutions with the chosen one being closest to the upper right corner where both fit and zero ratios are equal to 1. The optimal sparsity parameter for the age groups is $.51 \times \sqrt{21}$ (21 age groups), and the optimal sparsity parameter for the causes of death is $.31 \times \sqrt{19}$ (19 causes of death). The sparsity index from this analysis was equal to .473.

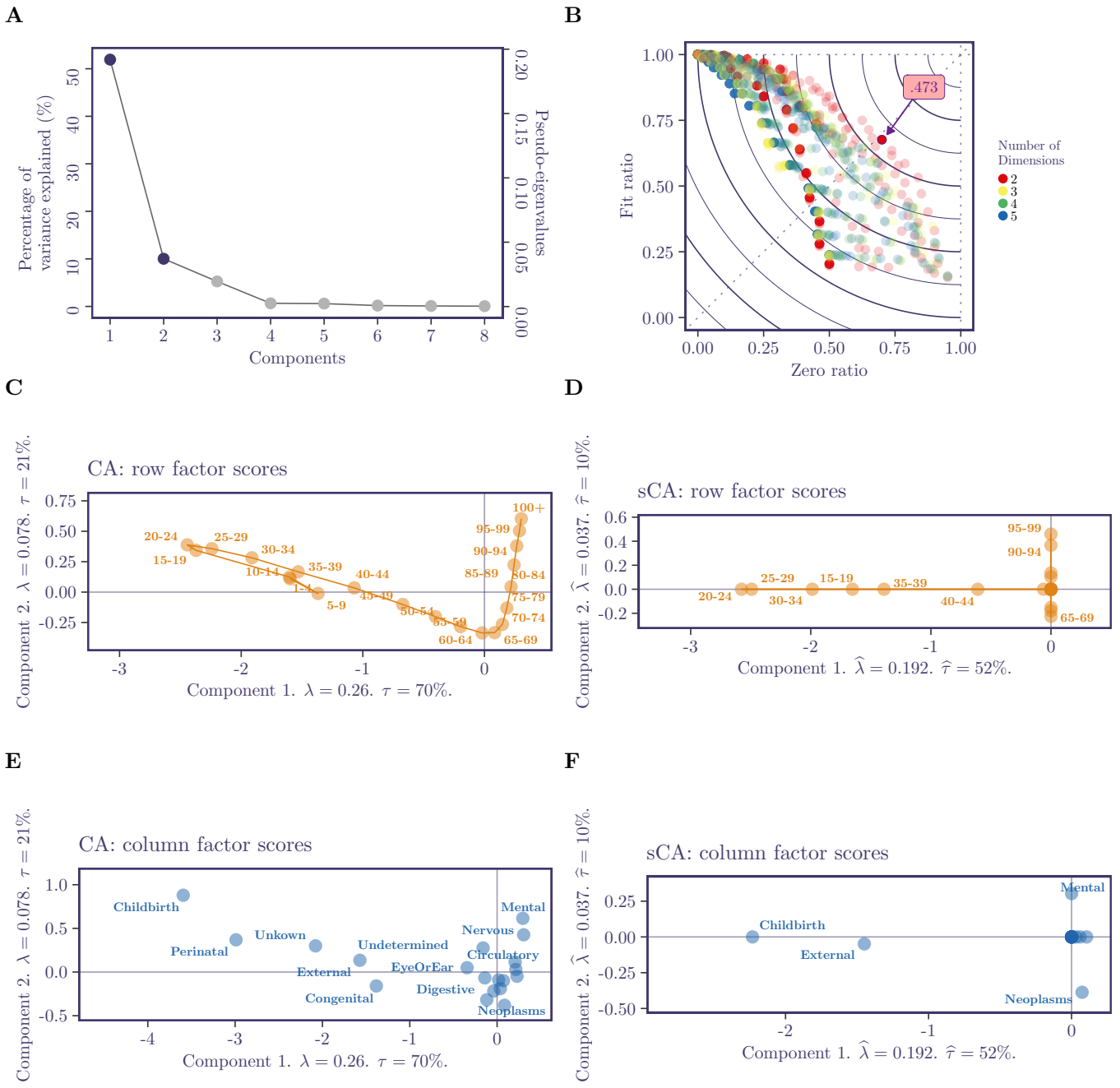

Figure 2. Results of CA and sCA. (A) shows the scree plot of sCA with the optimal number of components colored in purple. (B) shows the fit-to-zero-ratio plot and highlights the optimal solution that has the maximum sparsity index. (C) and (D) show the row factor scores (which represent different age ranges) from CA and sCA. (E) and (F) show the column factor scores (which represent different causes of death) from CA and sCA.

In CA, the first component has an eigenvalue of .26 which explains 70% of the inertia, and the second component has an eigenvalue of .08 which explains 21% of the variance. The row and the column factor scores show that the first

component is characterized by deaths between the late teens and twenties that are related to childbirth and deaths at a young age ($<$ 35 years old) that are related to congenital and perinatal conditions (see the horizontal axis in Figures 2C and E). The second component is characterized by deaths at older ages ($>$ 65 years old) that are mostly driven by malfunction in the nervous system such as Alzheimer's and Parkinson's diseases (see the vertical axis in Figures 2C and E). With sCA, the components give a clearer pattern that facilitates interpretation. The sparsified row and the column factor scores show that the first component is characterized by deaths in early adulthood (between 20–35) that are related to childbirth and external causes (e.g., suicide). The second component differentiates deaths between 60–80 years old, which relate to the causes of neoplasms (e.g., cancer), from deaths at 90 years old, which relate to mental conditions.

4.2. sDiSCA

4.2.1. Data

To demonstrate sparse DiSCA, we used a data set that counts the numbers of punctuation marks in works of authors from different times and origins. The texts were extracted from the Gutenberg Project using the R-`gutenbergr` package (Robinson, 2021). In this data set, we included authors from France ($N = 63$), the United Kingdom ($N = 61$), and the United States ($N = 36$) and from different periods (see Table 1). The data counted the number of occurrences of the following nine punctuation marks: comma (,), period (.), question mark (?), exclamation mark (!), colon (:), semicolon (;) apostrophe ($'$), quotation marks for both English (“ ") and French (« »), dashes (-), and M-dashes (—). We did not include the translated works and only considered the books written in the authors' original languages. We used DiSCA and sDiSCA to perform discriminant analysis on the eight author groups listed in Table 1.

Table 1

Numbers of authors in each group.

Origin	Time Period (centry)		
	18th and before	19th	20th and after
France	16	28	19
UK	11	28	22
US	14		22

Note. UK: United Kingdom; US: United States.

4.2.2. Results

The sDiSCA results are shown in Figure 3. Here, we consider a solution with 2 components because it gives the optimal results according to the sparsity index (Figure 3B). As shown in Figure 3B, this result is also the sparsest solution with the largest fit (closest to the upper right corner where both fit and zero ratios equal 1). The sparsity

parameter for the individuals is set to equal $.71 \times \sqrt{8}$ (8 author groups), and the optimal sparsity parameter for the punctuation marks is $.41 \times \sqrt{9}$ (9 punctuation marks). The sparsity index from this analysis is equal to .335.

The original and the sparsified component spaces are shown in Figure 3C–3F. Figure 3C shows the factor scores of the author groups from DiSCA, and Figure 3D shows the same results from sDiSCA. The individual authors are projected as supplementary observations onto the same components and are used to illustrate the stability of these group means by estimating their 95% bootstrap confidence intervals. When two confidence intervals overlap, the difference between the two groups is considered non-significant (with $\alpha = .05$). In DiSCA, the first component distinguishes the French-speaking authors from the English-speaking authors, and the second component distinguishes the English-speaking authors from different periods of time. By contrast, the French authors are more consistent across time.

The results from sDiSCA show a similar pattern in Figure 3D; the first component identifies only the three French groups of authors, and the second component identifies the oldest and the most recent groups of English authors. However, the bootstrap confidence intervals have quite a large variance—mostly because these intervals are derived from the supplementary projections of the authors with sparsification involved. While the sparsification algorithm sparsifies the number of contributing groups of each component, the group separations are, as a trade-off, no longer optimized, and thus results in supplementary projections are less segregated between groups.

The same trade-off is also reflected in the classification accuracy. In DiSCA, the discrimination between groups is measured by the accuracy of correct classifications. To classify observations, their supplementary factor scores are compared to the group factor scores and classified as belonging to the closest group. The accuracy rate of DiSCA is .44 and the accuracy rate of sDiSCA is .16. Although lower than for DiSCA, the accuracy is still above chance level (.125). The accuracy rate is higher with respect to the origins (DiSCA: .74; sDiSCA: .47; chance level: .33) with the French authors being classified most accurately (DiSCA: 1; sDiSCA: .68) as compared to the UK (DiSCA: .59; sDiSCA: .52) and the US (DiSCA: .56; sDiSCA: .27) authors.

Figure 3E shows the factor scores of the punctuation marks from plain DiSCA, and Figure 3F shows the same results from sDiSCA. The language effect on the first component is associated with the difference between how these authors punctuated quotation marks and apostrophes. This language effect is therefore consistent with the difference in how apostrophes are used differently in English (to represent possession) and French (for grammatical purposes). The time effect on the second component is associated with how authors used colons, semicolons, and commas (which connect sentences) versus how they used quotation marks, apostrophes, question, and exclamation marks (which end sentences). Therefore, the time effect could be related to how the style changes in English writing across time. Similar punctuation patterns are also shown in the results of sDiSCA which identified the quotation marks and the apostrophes as contributing most to the group differences.

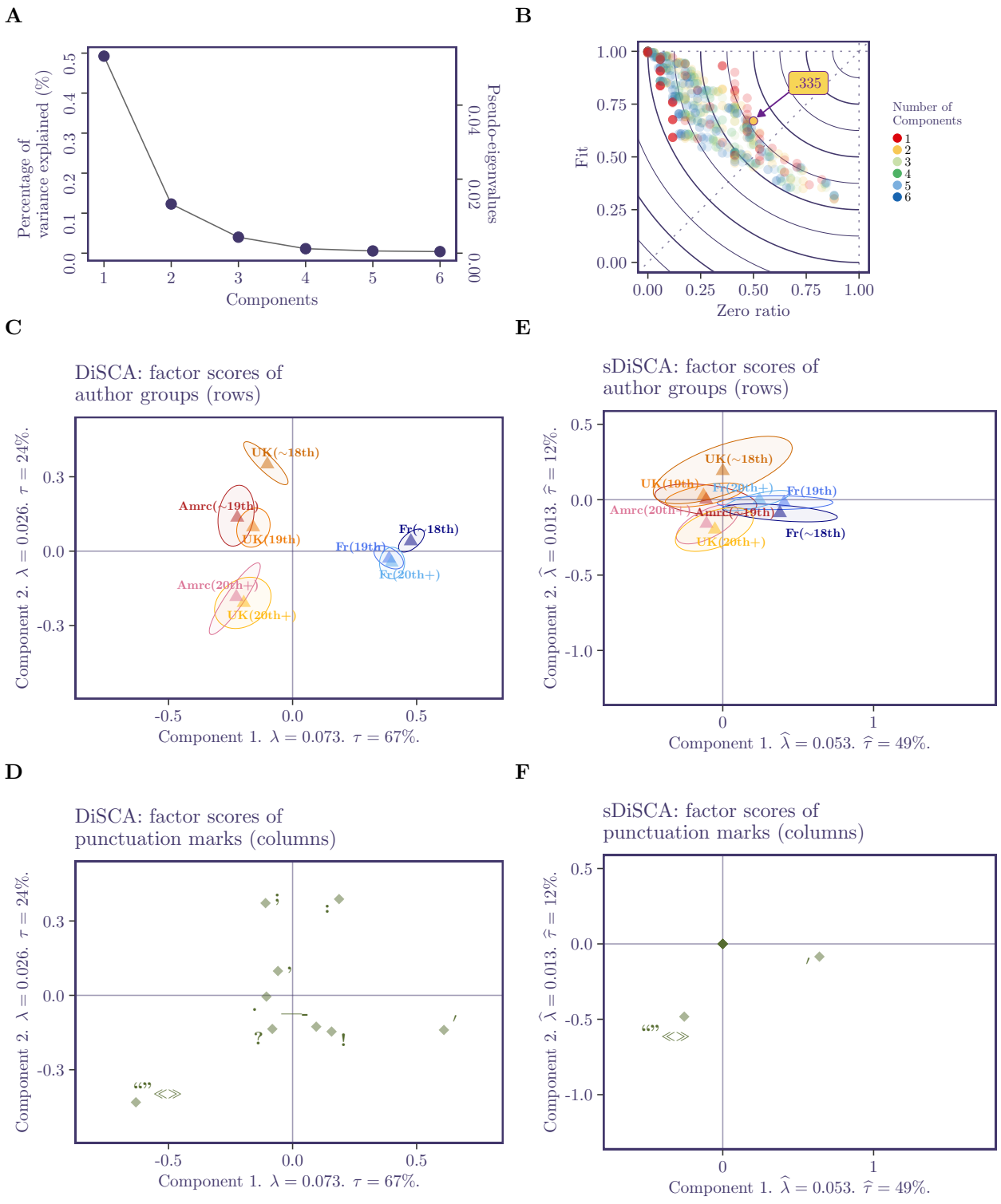

Figure 3. Results of DiSCA and sDiSCA. (A) shows the scree plot of sDiSCA with the optimal number of components. (B) shows the fit-to-zero-ratio plot and highlighted the optimal solution with the maximum sparsity index. (C) and (D) show the row factor scores (which represent the groups of authors) from DiSCA and sDiSCA. (E) and (F) show the column factor scores (which represent the punctuation marks) from DiSCA and sDiSCA.

4.3. sMCA

4.3.1. Data

To illustrate sMCA, we used a data set on the Chinese version of the Independent and Interdependent Self Scale (C-IISS) developed by Lu and Gilmour (2007). This data set describes 130 undergraduate students (77 females and 53 Males; $M_{\text{age}} = 19.49$, and $sd_{\text{age}} = 1.52$) from National Cheng Kung University. These participants signed written informed consents and received NTD 120 at the end of the experiment. The C-IISS comprised forty-two 7-point Likert scale questions (1 = strongly disagree; 7 = strongly agree). Among the 42 items, 21 of them measured independence (i.e., if one is aware of and values oneself as an individual) and the other 21 measured interdependence (i.e., how one values oneself and acts based on one's cohort). Before we analyzed the data with sMCA, because the results of MCA (and sMCA) will be driven by the rarity of an event, we binned the responses of each item into categories of comparable sizes (see Supplementary Figure G.1). The association patterns between these items are given in Supplementary Figure G.2. We analyzed the binned data with both MCA and sMCA, where we only sparsified the items. Although sparsifying the individuals (or both) is also possible, we did not sparsify them because the separation of individuals was not of interest in this study.

4.3.2. Results

The sMCA results are shown in Figure 4. For this data set, sMCA with 9 components gives the optimal results according to the sparsity index (Figure 4B). As shown in Figure 4C, this result is also the sparsest solution with the largest fit (closest to the upper right corner where both fit and zero ratios equal 1). The sparsity parameter for the individuals was set to $\sqrt{130}$ (i.e., no sparsity; 130 individuals), and the optimal sparsity parameter for the items is $.33 \times \sqrt{42}$ (42 item levels). The sparsity index from this analysis equals .377.

The plain and sparsified component spaces are shown in Figure 4D-4I. In plain MCA—with Benzécri's (1979) eigenvalue correction—the first component eigenvalue of .08 explains 72% of the inertia, and the second component with an eigenvalue of .01 explains 9% of the inertia. Because it is still unclear how such a correction should be applied to sMCA, we report here the uncorrected values directly from the GSVD for easier comparison between the two methods. Without Benzécri's correction, the first component from plain MCA with an eigenvalue of .30 explains 13.83% of the variance, and the second component with an eigenvalue of .12 explains 5.71% of the variance. The factor scores of the individuals are grouped according to their sex at birth, and the factor scores of the items are colored according to their corresponding category. The results showed that MCA generated components that could be difficult to explain given the complex pattern of loadings (see Figure 4D), whereas the first two components from sMCA distinguished items from different categories (see Figure 4F-4H). Specifically, the first component of sMCA identifies linear level effects of 5 questions that measure the level of independence; the second component of sMCA identifies linear level effects of 5 questions that measure the level of interdependence. The first component from sMCA with an eigenvalue of .07 explains 3.41% of the variance, and the second component with an eigenvalue of .06 explains 2.57% of the variance. Figures 4E and 4I show the factor scores of the individuals with the mean factor score of each sex group.

To examine group effect post-hoc, the stability of these group means is illustrated by their 95% bootstrap confidence intervals; when two confidence intervals overlap, the difference between the two groups is considered non-significant (with $\alpha = .05$) in MCA but significant in sMCA. In general, the individual factor scores from both analyses showed similar group separations with a marginal difference.

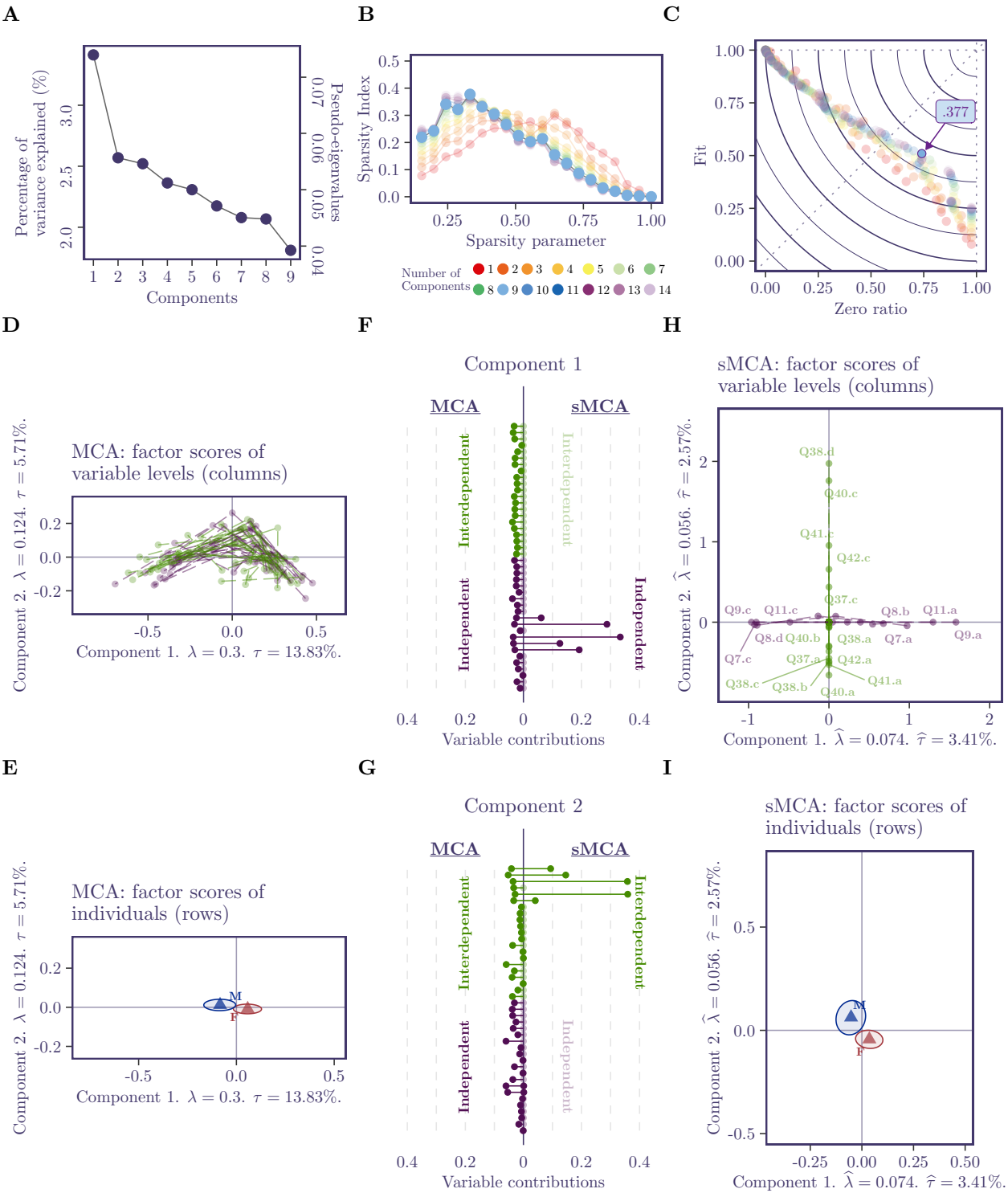

Figure 4. Results from MCA and sMCA. (A) shows the scree plot of sMCA with the optimal number of components. (B) and (C) show the fit-to-zero-ratio plot and highlights the optimal solution with the maximum sparsity index. (D) and (H) show the column factor scores (which represent variable levels) from MCA and sMCA with the levels of the same variables connected from low to high to illustrate the trend. Items measuring interdependent self are colored in green, and items measurng independent self are colored in purple. (F) and (G) show the variables that contribute to the two components of MCA and sMCA side by side. (E) and (I) show the mean row factor scores (which represent individuals) from MCA and sMCA with the blue triangle denoting the male group and the red triangle denoting the female group. The ellipses around the means illustrate the 95% bootstrap confidence intervals of the group means.

Table 2

Description of the groups for the Math questionnaire data

Domain	Short Name	Number of Items
basic algebraic skills	Algebra	8
basic arithmetic skills	Arith	5
categorization and ranges	CatRang	3
decimals, fractions, and percentages	DecFracPerc	12
visual understanding	Visual	2

4.4. sDiMCA

4.4.1. Data

The data we used to demonstrate DiMCA and sDiMCA were collected from undergraduate students enrolled in an introductory psychology statistics course taught by various instructors, at an urban public college in the northeast of the United States. The course covered descriptive statistics, hypothesis testing, and an overview of advanced statistical procedures. The Math Assessment for College Students (MACS; Rabin et al., 2018) was administered to 460 participants across five semesters, measuring basic mathematics skills through a 30-item paper-and-pencil test, which covered five general content domains (Table 2). Informed consent was obtained under an IRB-approved protocol and participants were not compensated. Demographic and academic performance data were also collected. The goal of the study was to examine the relationship between basic mathematics skills, demographic data, and academic performance.

The MACS questions took approximately 40 minutes and students completed the MACS during the first week of the semester. All 30 MACS items were graded with no partial credit, with each response recorded as 0 = incorrect and 1 = correct (scored by a single rater and re-scored by a second independent rater; Rabin et al., 2018). The course was computationally based, with students learning to perform statistical tests manually and use statistical software programs. Academic performance was evaluated based on the average score computed from three exams conducted in each semester. All exams included multiple-choice and problem-solving questions that covered basic statistics theory and applications. The average score was then categorized into a letter grade common to most undergraduate statistics courses, where: A = 90-–100%; B = 80–89%; C = 70–79%; D = 60—69%; and F = below 60%. For this illustration, A and B grades were grouped together as were D and F grades, resulting in a total of 3 groups (i.e., AB, C, DF).

4.4.2. Results

DiMCA and sDiMCA results are shown in Figure 5. For this data set, sMCA with 2 components gives the optimal non-unidimensional results according to the sparsity index (Figure 5B). As shown in Figure 5B, this result is also the sparsest solution with the largest fit (closest to the upper right corner where both fit and zero ratios equal 1). The sparsity parameter for the groups is set to equal $.79 \times \sqrt{5}$, and the optimal sparsity parameter for the items is $.57 \times \sqrt{60}$ (60 item levels). The sparsity index from this analysis equals .257.

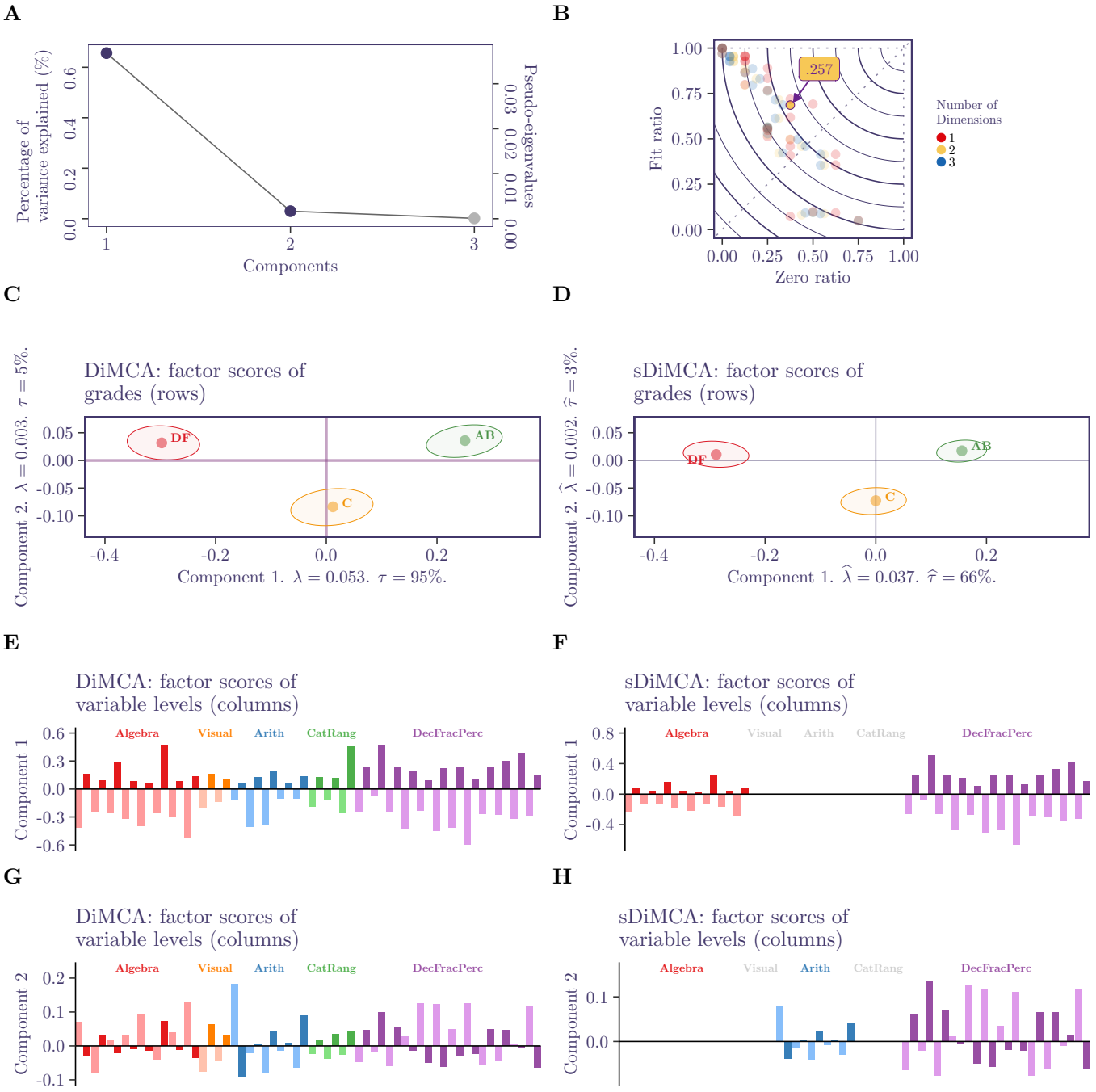

Figure 5. Results from DiMCA and sDiMCA. (A) scree plot of DiMCA with components to keep (dark purple). (B) fit-to-zero-ratio plot with optimal solution highlighted. (C) and (D) row factor scores from (respectively) DiMCA and sDiMCA. Ellipsoids show bootstrap derived confidence intervals. (E) to (H) factor scores for the variables colored by category for DiMCA (on the left) and sDiMCA (on the right)—only non-null values are shown.

As shown in Figure 5, both DiMCA and sDiMCA differentiated between AB-level and DF-level students along the first dimension, and this difference was driven by the overall number of correct and incorrect responses on the

MACS, where AB-level students had more correct responses and DF-level students had more incorrect responses. Specifically, DiMCA indicates that responses for all 30 MACS items reliably contribute to differences in performance, a pattern implying that DF-level students—compared to AB-level students—had an overall low performance across all basic domains of mathematics In contrast, sDiMCA reveals that differences in performance on particular items related to basic algebraic skills and decimals, fractions, and percentages most discriminated between AB-level students and DF-level students. These topics are usually covered in elementary and middle school and may not have been reviewed prior to college-level statistics. Therefore, students could be encouraged to take statistics earlier than later in college when basic mathematics skills are more likely to be remembered.

Based on MACS performance, certain students could be identified as "under-prepared" or "at risk" for poor outcomes in an introductory statistics course and might benefit from remediation before attempting courses that rely heavily on mathematics. Such remediation could be developed either as in-person or online formats with assignments completed independently or with a small learning group. Ideally, such efforts would provide opportunities for early success in introductory statistics courses through mastery of relevant pre-requisite mathematics skills.

In addition, both DiMCA and sDiMCA differentiated the C-level students from other grade levels along the second dimension, but DiMCA, once again, showed that responses for all 30 MACS items reliably contributed to this difference. However, sDiMCA revealed that C-level students were able to correctly answer specific subsets of items in basic arithmetic (e.g., order of operations) and decimals, fractions, and percentages (e.g., adding fractions) that differentiated them from DF-level students, but incorrectly answered enough items (e.g., rounding to the nearest decimal, decimal and percentage conversions) to differentiate them from the AB-level students. These results suggest that while C-level students are slightly better than DF-level students on certain concepts, these students might also benefit from remediation so that all students have the opportunity to begin the course with a similar level of mathematics proficiency.

5. Conclusion and discussion

In this paper, we extended the sparse GSVD introduced in Yu et al. (2023) to create the group-sparse GSVD (gsSVD) algorithm which keeps the orthogonality constraints of the GSVD while integrating sparsification with metric and group constraints. We applied the gsGSVD to sparsify CA, MCA, and their respective discriminant analysis versions: DiSCA and DiMCA. We illustrated these sparsification methods and compared their analytical merits on four real data sets. We also integrated group constraints into the sparsification problem—an essential property for categorical data analysis where variables are represented by blocks of columns. These group constraints could also be applied to different situations such as for data with *a priori* groups of variables.

This new gsGSVD algorithm seeks optimum solutions that satisfy strong constraints such as orthogonality and sparsity. Interestingly, our results also showed that sparsification can be interpreted as a form of cluster analysis performed on the rows or the columns of the data matrix—an approach akin to, for example, spectral clustering which

partitions the variables based on their singular vectors (Kannan et al., 2000) or graph analysis (Spielman and Teng, 2011). Overall, we demonstrated how this new algorithm provides new multivariate tools to explore the complex structures of qualitative data.

To sparsify solutions while maintaining orthogonality between components, we used POCS to integrate two sets of strong constraints: one for orthogonality and one for sparsification. However, in some cases, these constraints can be so strong that they may not be all satisfied together. For example, to sparsify the solution while keeping the components orthogonal, we project the data onto the orthogonality constraints first and the sparsification constraints last. This approach guarantees that sparsity and orthogonality are satisfied to a high level of precision i.e., (below 1e-10). In practice, it is also possible to switch the order of projections and project onto the orthogonality constraints last. This order of projections prioritizes orthogonality over sparsity. It is worth noting that, sometimes, the solution of prioritizing different constraints could lead to different results. In certain circumstances, meeting both orthogonality and sparsity constraints is not feasible. In such cases, the prioritized constraint will be satisfied at the expense of the other.

It is worth noting that the dimensions derived from the sparse SVD algorithm might not always be obtained in decreasing order of explained variance—a problem already present in Witten et al. (2009). The original order should be kept to implement the orthogonality constraints and for the transition formulas to work correctly. However, for convenience and to follow traditions, the current output of the R-implementation reorders the dimensions according to their variance.

Additionally, as is done by (Witten et al., 2009) and (Guillemot et al., 2019), to make Algorithm 1 a convex optimization problem with convex constraints, the constraints on the (group-)$\mathcal{L}_1$- and $\mathcal{L}_2$-norms used are inequality constraints—an interpretation that could hinder the interpretability of the results. For example, when the $\mathcal{L}_2$-norms of some loadings are less than 1. In practice, however, these constraints are saturated, meaning that it is rarely the case that the $\mathcal{L}_2$-norms of the resulting pseudo generalized singular vectors are not exactly 1, or that their $\mathcal{L}_1$-norms are not exactly the given sparsity parameters. For cases when the constraints are unsaturated (i.e., they are not compatible), the solutions will not be unique and could be unstable.

The proposed sparse methods still require future developments on solutions to preserve more CA-MCA-related properties and on inference analysis to evaluate the stability and validity of the sparse solution. The current work also opens avenues to explore the properties of the POCS projecting operators such as the projection of supplementary elements, which currently uses approximations.

Overall, this study presents an exciting foundation for refining and expanding the use of sparsification techniques. Future avenues could extend the current methods to two data table analyses such as Partial Least Squares Correlation (PLSC) and its CA-like extension PLS-CA and PLS-MCA. Future directions could also incorporate the consideration of hierarchical structures of variables or observations such as overlapping groups of grouped variables, exemplified in Single Nucleotide Polymorphism (SNP) data structured into pathways.

6. Acknowledgements

JCY receives funding from the Discovery Fund postdoctoral fellowship of the Centre of Addiction and Mental Health

LR and AK received funding from the PSC-CUNY TRADA Award (62058-00 50)

LR received funding from NSF Research Experiences for Undergraduates (REU) Award (2050755)

References

Abdi, H., 2007. Discriminant correspondence analysis, in: Salkind, N.J. (Ed.), Encyclopedia of measurement and statistics, Sage. pp. 270–275.

Abdi, H., Béra, M., 2014. Correspondence analysis, in: Alhajj, R., Rokne, J. (Eds.), Encyclopedia of Social Network Analysis and Mining, Springer. pp. 275–284.

Abdi, H., di Caccio, A., Saporta, G., 2024. Old and new perspectives on optimal scaling, in: Beh, Eric, J., Lombardo, R., Clavel, Jose, G. (Eds.), Analysis of Categorical Data from Historical Perspectives. Springer Singapore. chapter 9, pp. 1–24.

Abdi, H., Valentin, D., 2007. Multiple correspondence analysis, in: Salkind, N. (Ed.), Encyclopedia of measurement and statistics, Sage. pp. 651–66.

Benzécri, J.P., 1979. Sur le calcul des taux d'inertie dans l'analyse d'un questionnaire. Cahiers de l'Analyse des Données 4, 377–378.

Benzécri, J.P., et al., 1973. L'analyse des données. volume 2. Dunod Paris.

van den Berg, E., Schmidt, M., Friedlander, M.P., Murphy, K., 2008. Group sparsity via linear-time projection. Department of Computer Science, University of British Columbia Technical Report .

Bernard, A., Guinot, C., Saporta, G., 2012. Sparse principal component analysis for multiblock data and its extension to sparse multiple correspondence analysis, in: Proceedings of 20th International Conference on Computational Statistics (COMPSTAT 2012), pp. 99–106.

Cadima, J., Jolliffe, I.T., 1995. Loading and correlations in the interpretation of principle components. Journal of applied Statistics 22, 203–214.

Cattell, R.B., 1978. The scientific use of factor analysis in behavioral and life sciences .

Combettes, P., 1993. The foundations of set theoretic estimation. Proceedings of the IEEE 81, 182–208.

Efron, B., 2020. Prediction, estimation, and attribution. Journal of the American Statistical Association 115, 636–655.

Efron, B., Hastie, T., 2016. Computer age statistical inference. Cambridge University Press.

Escofier, B., 1969. L'analyse des correspondences. Bulletin du Bureau Universitaire de Recherche Opé'rationelle 11, 1–48.

Escofier, B., 1979. Une représentation des variables dans l'analyse des correspondances multiples. Revue de Statistique Appliquée 27, 37–47.

Fichet, B., 2009. Metrics of L_p-type and distributional equivalence principle. Advances in data analysis and classification 3, 305.

Greenacre, M., 1984. Theory and applications of correspondence analysis. London (UK) Academic Press.

Guillemot, V., Beaton, D., Gloaguen, A., Löfstedt, T., Levine, B., Raymond, N., Tenenhaus, A., Abdi, H., 2019. A constrained singular value decomposition method that integrates sparsity and orthogonality. PLoS ONE 14, e0211463.

Hastie, T., Tibshirani, R., Friedman, J., 2009. The elements of statistical learning: data mining, inference, and prediction. Springer Science & Business Media.

Jolliffe, I.T., Trendafilov, N.T., Uddin, M., 2003. A modified principal component technique based on the lasso. Journal of Computational and Graphical Statistics 12, 531–547.

Jolliffe, I.T., Uddin, M., 2000. The simplyfied component technique: An alternative to rotated principal components. Journal of Computational and Graphical Statistics 9, 689–710.

Journée, M., Nesterov, Y., Richtárik, P., Sepulchre, R., 2010. Generalized power method for sparse principal component analysis. Journal of Machine Learning Research 11, 517–553.

Kannan, R., Vempala, S.S., Vetta, A., 2000. On clusterings-good, bad and spectral. Proceedings 41st Annual Symposium on Foundations of Computer Science , 367–377URL: https://api.semanticscholar.org/CorpusID:61731027.

Lebart, L., Morineau, A., Warwick, K.M., 1984. Multivariate descriptive statistical analysis : correspondence analysis and related techniques for large matrices. Wiley.

Liu, R., Niang, N., Saporta, G., Wang, H., 2023. Sparse correspondence analysis for large contingency tables. Advances in Data Analysis and Classification , 1–20URL: https://link.springer.com/article/10.1007/s11634-022-00531-5, doi:10.1007/S11634-022-00531-5/FIGURES/8.

Lu, L., Gilmour, R., 2007. Developing a new measure of independent and interdependent views of the self. Journal of Research in Personality 41, 249–257.

Mackey, L., 2009. Deflation methods for sparse PCA, in: Koller, D., Schuurmans, D., Bengio, Y., Bottou, L. (Eds.), Advances in Neural Information Processing Systems, Curran Associates, Inc.. pp. 1017–1024. URL: https://proceedings.neurips.cc/paper/2008/file/85d8ce590ad8981ca2c8286f79f59954-Paper.pdf.

Mori, Y., Kuroda, M., Makino, N., 2016. Sparse Multiple Correspondence Analysis, in: Nonlinear Principal Component Analysis and Its Applications. Springer Singapore. chapter 5, pp. 47–56. doi:10.1007/978-981-10-0159-8_5.

Qi, X., Luo, R., Zhao, H., 2013. Sparse principal component analysis by choice of norm. Journal of multivariate analysis 114, 127–160.

Rabin, L., Fink, L., Krishnan, A., Fogel, J., Berman, L., Bergdoll, R., 2018. A Measure of Basic Math Skills for Use With Undergraduate Statistics Students: the MACS. Statistics Education Research Journal 17, 179–195. URL: https://iase-web.org/ojs/SERJ/article/view/165, doi:10.52041/SERJ.V17I2.165.

Robinson, D., 2021. gutenbergr: Download and Process Public Domain Works from Project Gutenberg. URL: https://CRAN.R-project.org/package=gutenbergr. r package version 0.2.1.

Saporta, G., 2011. Probabilités, Analyse des Données et Statistique. 3rd ed., Technip, Paris, France.

Spielman, D.A., Teng, S.H., 2011. Spectral sparsification of graphs. SIAM Journal on Computing 40, 981–1025.

Thurstone, L.L., 1935. The vectors of mind: Multiple-factor analysis for the isolation of primary traits. University of Chicago Press.

Thurstone, L.L., 1947. Multiple-factor analysis; a development and expansion of the vectors of mind. .

Tibshirani, R., 1996. Regression shrinkage and selection via the lasso. Journal of the Royal Statistical Society: Series B (Methodological) 58, 267–288.

Trendafilov, N., Gallo, M., 2021. Multivariate data analysis n matrix manifolds. Springer, Genève, Switzerland.

Trendafilov, N.T., 2014. From simple structure to sparse components: a review. Computational Statistics 29, 431–454.

Trendafilov, N.T., Adachi, K., 2015. Sparse versus simple structure loadings. Psychometrika 80, 776–790.

Trendafilov, N.T., Fontanella, S., Adachi, K., 2017. Sparse Exploratory Factor Analysis. Psychometrika 82, 778–794. doi:10.1007/s11336-017-9575-8.

Trendafilov, N.T., Jolliffe, I.T., 2006. Projected gradient approach to the numerical solution of the scotlass. Computational Statistics & Data Analysis 50, 242–253.

Witten, D.M., Tibshirani, R., Hastie, T., 2009. A penalized matrix decomposition, with applications to sparse principal components and canonical correlation analysis. Biostatistics 10, 515–534.

World Health Organization, W., 2019. The ICD-10 classification of mental and behavioural disorders. World Health Organization, Genève, Switzerland. URL: https://icd.who.int/browse10/2019/en/.

Yu, J.C., Gómez-Corona, C., Abdi, H., Guillemot, V., 2023. Sparse multiple factor analysis, sparse statis, and sparse distatis with applications to sensory evaluation. Journal of Chemometrics n/a, e3443. doi:https://doi.org/10.1002/cem.3443.

Yuan, M., Lin, Y., 2006. Model selection and estimation in regression with grouped variables. Journal of the Royal Statistical Society: Series B (Statistical Methodology) 68, 49–67.

Zou, H., Hastie, T., 2005. Regularization and variable selection via the elastic net. Journal of the royal statistical society: series B (statistical methodology) 67, 301–320.

Zou, H., Hastie, T., Tibshirani, R., 2006. Sparse principal component analysis. Journal of computational and graphical statistics 15, 265–286.

Appendix A. CA and inertia

Recall that, for an $I \times J$ contingency table, the independence χ^2 statistic is computed as:

$$\chi^2 = \sum_{i,j} \frac{(\text{Observed}_{i,j} - \text{Expected}_{i,j})^2}{\text{Expected}_{i,j}} \tag{A.1}$$

or, in matrix notation, the χ^2 is associated to the matrix $\mathbf{X}$ (with the notations from Equations 2 and 3) and computed as:

$$\frac{1}{N}\chi^2 = \mathsf{trace}\left(\mathbf{D_c}^{-\frac{1}{2}}\mathbf{X}^\top\mathbf{D_r}^{-1}\mathbf{X}\mathbf{D_c}^{-\frac{1}{2}}\right) = \mathsf{trace}\left(\mathbf{D_r}^{-\frac{1}{2}}\mathbf{X}\mathbf{D_c}^{-1}\mathbf{X}^\top\mathbf{D_r}^{-\frac{1}{2}}\right). \tag{A.2}$$

From the GSVD, the inertia computed from the row factors $\mathbf{F}$ gives $\frac{1}{N}\chi^2$:

$$\begin{aligned}
&\mathsf{trace}\left(\mathbf{F}^\top\mathbf{D_r}\mathbf{F}\right)\\
&= \mathsf{trace}\left(\mathbf{V}^\top\mathbf{D_c}^{-1}\mathbf{X}^\top\mathbf{D_r}^{-1}\mathbf{D_r}\mathbf{D_r}^{-1}\mathbf{U}\boldsymbol{\Delta}\right)\\
&= \mathsf{trace}\left(\mathbf{D_c}^{-1}\mathbf{X}^\top\mathbf{D_r}^{-1}\mathbf{U}\boldsymbol{\Delta}\mathbf{V}^\top\right)\\
&= \mathsf{trace}\left(\mathbf{D_c}^{-1}\mathbf{X}^\top\mathbf{D_r}^{-1}\mathbf{X}\right)\\
&= \mathsf{trace}\left(\mathbf{D_c}^{-\frac{1}{2}}\mathbf{X}^\top\mathbf{D_r}^{-1}\mathbf{X}\mathbf{D_c}^{-\frac{1}{2}}\right)\\
&= \frac{1}{N}\chi^2,
\end{aligned} \tag{A.3}$$

and so does the inertia computed from the column factors $\mathbf{G}$:

$$\begin{aligned}
&\mathsf{trace}\left(\mathbf{G}^\top\mathbf{D_c}\mathbf{G}\right)\\
&= \mathsf{trace}\left(\mathbf{U}^\top\mathbf{D_r}^{-1}\mathbf{X}\mathbf{D_c}^{-1}\mathbf{D_c}\mathbf{D_c}^{-1}\mathbf{V}\boldsymbol{\Delta}\right)\\
&= \mathsf{trace}\left(\mathbf{D_r}^{-1}\mathbf{X}\mathbf{D_c}^{-1}\mathbf{V}\boldsymbol{\Delta}\mathbf{U}^\top\right)\\
&= \mathsf{trace}\left(\mathbf{D_r}^{-1}\mathbf{X}\mathbf{D_c}^{-1}\mathbf{X}^\top\right)\\
&= \mathsf{trace}\left(\mathbf{D_r}^{-\frac{1}{2}}\mathbf{X}\mathbf{D_c}^{-1}\mathbf{X}^\top\mathbf{D_r}^{-\frac{1}{2}}\right)\\
&= \frac{1}{N}\chi^2.
\end{aligned} \tag{A.4}$$

Appendix B. The SVD and the generalized SVD (GSVD)

The SVD decomposes the data matrix $\mathbf{X}$ into three matrices:

$$\mathbf{X} = \mathbf{P}\boldsymbol{\Delta}\mathbf{Q}^\top \quad \text{such that} \quad \mathbf{P}^\top\mathbf{P} = \mathbf{Q}^\top\mathbf{Q} = \mathbf{I}, \tag{B.1}$$

where $\mathbf{P}$ (respectively $\mathbf{Q}$) is the $I \times L$ (respectively $J \times L$) matrix of the left (respectively right) singular vectors, and $\boldsymbol{\Delta}$ is a diagonal matrix with singular values δs stored on its diagonal. The SVD solves the following maximization problem:

$$\begin{aligned} &\underset{\mathbf{p}_\ell,\mathbf{q}_\ell}{\arg\max} \left(\delta_\ell = \mathbf{p}_\ell^\top \mathbf{X}\mathbf{q}_\ell\right) \quad \text{subject to} \\ &\begin{cases} \mathbf{p}_\ell^\top\mathbf{p}_\ell &= 1, \\ \mathbf{q}_\ell^\top\mathbf{q}_\ell &= 1, \end{cases} \text{and, for any } \ell \neq \ell', \quad \begin{cases} \mathbf{p}_\ell^\top\mathbf{p}_{\ell'} &= 0. \\ \mathbf{q}_\ell^\top\mathbf{q}_{\ell'} &= 0. \end{cases} \end{aligned} \tag{B.2}$$

Here, δ_ℓ is the ℓth singular value and is associated to the ℓth left (respectively right) singular vector $\mathbf{p}_\ell$ and $\mathbf{q}_\ell$.

Similar to the SVD, the GSVD also decomposes $\mathbf{X}$ into three matrices but with row and column metric matrices included in the constraints:

$$\mathbf{X} = \mathbf{U}\boldsymbol{\Delta}\mathbf{V}^\top \quad \text{such that} \quad \mathbf{U}^\top\mathbf{M}\mathbf{U} = \mathbf{V}^\top\mathbf{W}\mathbf{V} = \mathbf{I}, \tag{B.3}$$

where $\mathbf{U}$ (respectively $\mathbf{V}$) is the matrix of the left (respectively right) generalized singular vectors, $\mathbf{M}$ (respectively $\mathbf{W}$) is the row (respectively column) metric matrix represented by a positive definite matrix. The GSVD solves the following maximization problem:

$$\begin{aligned} &\underset{\mathbf{p}_\ell,\mathbf{q}_\ell}{\arg\max} \left(\delta_\ell = \mathbf{u}_\ell^\top \mathbf{X}\mathbf{v}_\ell\right) \quad \text{subject to} \\ \text{subject to} \quad &\begin{cases} \mathbf{u}_\ell^\top\mathbf{M}\mathbf{u}_\ell &= 1, \\ \mathbf{v}_\ell^\top\mathbf{W}\mathbf{v}_\ell &= 1, \end{cases} \text{and, for any } \ell \neq \ell', \quad \begin{cases} \mathbf{u}_\ell^\top\mathbf{M}\mathbf{u}_{\ell'} &= 0. \\ \mathbf{v}_\ell^\top\mathbf{W}\mathbf{v}_{\ell'} &= 0. \end{cases} \end{aligned} \tag{B.4}$$

The maximization problem of the GSVD is equivalent to the following SVD of the weighted $\mathbf{X}$ (denoted by $\widetilde{\mathbf{X}}$), where

$$\begin{aligned} \widetilde{\mathbf{X}} = \mathbf{M}^{\frac{1}{2}}\mathbf{X}\mathbf{W}^{\frac{1}{2}} &= \mathbf{P}\boldsymbol{\Delta}\mathbf{Q}^\top \\ \text{such that} \quad \mathbf{P}^\top\mathbf{P} &= \mathbf{Q}^\top\mathbf{Q} = \mathbf{I}, \end{aligned} \tag{B.5}$$

with

$$\begin{cases} \mathbf{U} &= \mathbf{M}^{-\frac{1}{2}}\mathbf{P} \\ \mathbf{V} &= \mathbf{W}^{-\frac{1}{2}}\mathbf{Q} \end{cases} \quad \text{such that} \quad \mathbf{U}^\top\mathbf{M}\mathbf{U} = \mathbf{V}^\top\mathbf{W}\mathbf{V} = \mathbf{I}. \tag{B.6}$$

Appendix C. Properties of CA, MCA, DiSCA, and DiMCA

Because of the specific preprocessing steps and the metric constraints, CA (and therefore MCA, DiSCA, and DiMCA) has several specific properties (Escofier, 1969; Greenacre, 1984).

Property C.1. *Transition formulas: The row factor scores can be computed from the column factor scores and vice versa.*

CA/MCA/DiSCA/DiMCA analyze the rows and columns symmetrically; therefore, the row (respectively column) factors can be obtained from the data and the column (respectively row) factors by a transition formula. Transition formulas can be derived from Equation 11: by substituting the $\mathbf{D_c^{-1}V}$ of $\mathbf{F}$,

$$\mathbf{F} = \mathbf{D_r^{-1}XD_c^{-1}V}, \quad \text{with} \quad \mathbf{D_c^{-1}V} = \mathbf{G\Delta^{-1}} \tag{C.1}$$

and the $\mathbf{D_r^{-1}U}$ of $\mathbf{G}$,

$$\mathbf{G} = \mathbf{D_c^{-1}X^\top D_r^{-1}U}, \quad \text{with} \quad \mathbf{D_r^{-1}U} = \mathbf{F\Delta^{-1}}, \tag{C.2}$$

$\mathbf{F}$ can be computed from $\mathbf{G}$ by

$$\mathbf{F} = \mathbf{D_r^{-1}XG\Delta^{-1}} \tag{C.3}$$

and $\mathbf{G}$ can be computed from $\mathbf{F}$ by

$$\mathbf{G} = \mathbf{D_c^{-1}X^\top F\Delta^{-1}}. \tag{C.4}$$

Property C.2. *Supplementary projections: Equations C.3 and C.4 can be used to estimate the factor scores from a supplementary, or called out-of-sample, row (respectively column) that is represented by the same set of columns (respectively rows).*

The factor score of a supplementary row $\mathbf{i}_{\text{sup}}$ (denoted $\mathbf{f}^*_{\text{sup}}$) is computed with an equation similar to Equation C.3:

$$\mathbf{f}^*_{\text{sup}} = \left(\mathbf{i}^\top_{\text{sup}}\mathbf{1}\right)^{-1}\mathbf{i}^\top_{\text{sup}}\mathbf{G\Delta^{-1}}. \tag{C.5}$$

The factor score of a supplementary column $\mathbf{j}_{\text{sup}}$ (denoted $\mathbf{g}^*_{\text{sup}}$ is computed by a similar equation to Equation C.4:

$$\mathbf{g}^*_{\text{sup}} = \left(\mathbf{1}^\top\mathbf{j}_{\text{sup}}\right)^{-1}\mathbf{j}^\top_{\text{sup}}\mathbf{F\Delta^{-1}}. \tag{C.6}$$

Geometrically, these factor scores project the supplementary rows (or column) onto the component space built by the original data.

Property C.3. *Distributional equivalence: Identical rows (or columns) can be replaced by their sum without affecting the results.*

Because CA and MCA analyze the frequencies of the occurrences, two rows (or two columns) that are proportional to each other become identical after the preprocessing steps. These identical rows (or columns) can be represented by *two* coincident points in the component space, and the two points can be merged into *one* with the sum of the original weights (Fichet, 2009; Benzécri et al., 1973; Greenacre, 1984). In addition, merging these two points does not change the geometry of the component space.

Property C.4. *Barycentric projection: Row and column factor scores, have barycenters of 0.*

The row and the column factor scores of CA/MCA/DiSCA/DiMCA share a common barycenter (i.e., weighted mean) of 0; Formally

$$\frac{1}{I}\mathbf{r}^\top \mathbf{f}_\ell = \frac{1}{J}\mathbf{c}^\top \mathbf{g}_\ell = 0. \tag{C.7}$$

Specifically in MCA, for each of the K variables, the (column) factor scores of its levels will have a weighted mean of zero:

$$\sum_{j=1}^{J_k} c_{j,k}\mathbf{g}_{j,k,\ell} = 0, \tag{C.8}$$

where $c_{j,k}$ is the column weight for the jth level of the kth variable, and $\mathbf{g}_{j,k,\ell}$ is the factor scores of the jth level of the kth variable on the ℓth component. In addition, for all observations that belong to this variable level, their mean (row) factor score will equal the (column) factor score of this variable level.

Property C.5. *The embedded solution: in CA, the GSVD of the non-centered matrix (i.e.,* $\mathbf{Z}$*) will have the first generalized singular value of 1, the first left generalized singular vector of* $\mathbf{r}$*, and the first right generalized singular vector of* $\mathbf{c}$*. In addition, the following components will be equivalent to the GSVD of the matrix* $\mathbf{X}$*.*

The embedded solution holds because the GSVD in CA (Equation 4) can be rewritten as:

$$\begin{aligned} \mathbf{X} = \mathbf{Z} - \mathbf{r}\mathbf{c}^\top = \mathbf{U}\boldsymbol{\Delta}\mathbf{V}^\top = \sum_{\ell=1}^{L} \delta_\ell \mathbf{u}_\ell \mathbf{v}_\ell^\top \\ \text{under the constraints} \quad \mathbf{U}^\top \mathbf{D}_\mathbf{r}^{-1}\mathbf{U} = \mathbf{V}^\top \mathbf{D}_\mathbf{c}^{-1}\mathbf{V} = \mathbf{I} \end{aligned} \tag{C.9}$$

which gives

$$\begin{aligned} \mathbf{Z} = \mathbf{r}\mathbf{c}^\top + \mathbf{U}\boldsymbol{\Delta}\mathbf{V}^\top = 1 \times \mathbf{r}\mathbf{c}^\top + \sum_{\ell=2}^{L} \delta_\ell \mathbf{u}_\ell \mathbf{v}_\ell^\top \\ \text{under the constraints} \quad \mathbf{U}^\top \mathbf{D}_\mathbf{r}^{-1}\mathbf{U} = \mathbf{V}^\top \mathbf{D}_\mathbf{c}^{-1}\mathbf{V} = \mathbf{I}. \end{aligned} \tag{C.10}$$

Therefore, when the non-centered data $\mathbf{Z}$ is analyzed, the first generalized singular value δ_1 equals 1, the first left generalized singular vector $\mathbf{u}_1$ equals $\mathbf{r}$, and the first right generalized singular vector $\mathbf{v}_1$ equals $\mathbf{c}$. With $\mathbf{r}\mathbf{c}^\top$ computing the *expected* frequencies of $\mathbf{Z}$ under independence, the CA of $\mathbf{X}$, where $\mathbf{X} = \mathbf{Z} - \mathbf{r}\mathbf{c}^\top$, analyzes the deviation of the *observed* data (i.e., $\mathbf{Z}$) from the independence (i.e., $\mathbf{r}\mathbf{c}^\top$).

Property C.6. *The asymmetric projection: The row and column factor scores of each component can be scaled to have either a variance of 1 or a variance of the associated eigenvalue. When the row and the column factor scores are scaled differently (i.e., one to have a variance of 1 with the other having a variance of the eigenvalue), they are projected asymmetrically.*

In the CA/MCA/DiSCA framework, the rows and columns are analyzed symmetrically and the extracted components can be seen from the perspective of the rows or of the columns. From the perspective of the rows, the component space is defined by the row factor scores (denoted by $\widetilde{\mathbf{F}}$) which are computed as:

$$\widetilde{\mathbf{F}} = \mathbf{D_r}^{-1}\mathbf{U} \quad \text{with its variance} \quad \widetilde{\mathbf{F}}^\top \mathbf{D_r} \widetilde{\mathbf{F}} = \mathbf{I}. \tag{C.11}$$

The columns can then be projected onto this component space as $\mathbf{G}$:

$$\mathbf{G} = \mathbf{D_c}^{-1}\mathbf{V}\boldsymbol{\Delta} \quad \text{with its variance} \quad \mathbf{G}^\top \mathbf{D_c} \mathbf{G} = \boldsymbol{\Lambda}. \tag{C.12}$$

Because the columns factor scores are projected onto this space and scaled differently from the row factor scores, this projection is *asymmetric*.

From the perspective of the columns, the component space is defined by the column factor scores (denoted by $\widetilde{\mathbf{G}}$) which are computed as:

$$\widetilde{\mathbf{G}} = \mathbf{D_c}^{-1}\mathbf{V} \quad \text{with its variance} \quad \widetilde{\mathbf{G}}^\top \mathbf{D_c} \widetilde{\mathbf{G}} = \mathbf{I}. \tag{C.13}$$

The asymmetric projection of the rows onto this space can then be computed as $\mathbf{F}$:

$$\mathbf{F} = \mathbf{D_r}^{-1}\mathbf{U}\boldsymbol{\Delta} \quad \text{with its variance} \quad \mathbf{F}^\top \mathbf{D_r} \mathbf{F} = \boldsymbol{\Lambda}. \tag{C.14}$$

According to Property C.5, because the first generalized singular value of the uncentered matrix equals 1, it is the maximum amount of variance any given component can have. When the factor scores of a component has a variance of 1, these factor scores span the entire space—called *simplex*—of the data. From Property C.4, the simplex defined by the row and the simplex defined by the column factors share the same *barycenter*. When one is used to define the simplex, the other can be projected asymmetrically onto this simplex where the distance between any two factor scores (including the distance between a row factor score and a column factor score) is meaningful. In contrast, when both the rows and the columns are symmetrically projected (as $\mathbf{F}$ and $\mathbf{G}$), only the distances within the same set are meaningful.

Appendix D. Transition formulas with and without sparsification

We derive the transition formulas for row and column factor scores, for regular and sparse CA-related methods. We provide a step-by-step breakdown of these derivations, highlighting specifically where the projection operators introduce non-linearity, leading to sparsity.

The original transition formulas are derived as follows for row ($\mathbf{f}$) and column ($\mathbf{g}$) factor scores:

$$\begin{aligned}
\mathbf{f}_\ell =& \mathbf{D}_\mathbf{r}^{-1}\mathbf{u}_\ell\delta_\ell \\
=& \mathbf{D}_\mathbf{r}^{-1}(\mathbf{U}\boldsymbol{\Delta}\mathbf{V}^\top)\mathbf{D}_\mathbf{c}^{-1}\mathbf{v}_\ell \\
=& \mathbf{D}_\mathbf{r}^{-1}\mathbf{X}\mathbf{D}_\mathbf{c}^{-1}\mathbf{v}_\ell \\
=& \mathbf{D}_\mathbf{r}^{-1}(\mathbf{Z}-\mathbf{r}\mathbf{c}^\top)\mathbf{D}_\mathbf{c}^{-1}\mathbf{v}_\ell \\
=& \mathbf{D}_\mathbf{r}^{-1}\mathbf{Z}\mathbf{D}_\mathbf{c}^{-1}\mathbf{v}_\ell \\
=& \mathbf{R}\mathbf{D}_\mathbf{c}^{-1}\mathbf{v}_\ell \\
=& \mathbf{D}_\mathbf{r}^{-1}\mathbf{Z}\mathbf{g}_\ell\delta_\ell^{-1},
\end{aligned} \tag{D.1}$$

where $\mathbf{Z}$ is the contingency table, $\mathbf{X}$ is the probability matrix, and $\mathbf{R}$ is the row profiles where $\mathbf{R} = \mathbf{D}_\mathbf{r}^{-1}\mathbf{Z}$ with each row of $\mathbf{R}$ sums to 1;

$$\begin{aligned}
\mathbf{g}_\ell =& \mathbf{D}_\mathbf{c}^{-1}\mathbf{v}_\ell\delta_\ell \\
=& \mathbf{D}_\mathbf{c}^{-1}(\mathbf{V}\boldsymbol{\Delta}\mathbf{U}^\top)\mathbf{D}_\mathbf{r}^{-1}\mathbf{u}_\ell \\
=& \mathbf{D}_\mathbf{c}^{-1}\mathbf{X}\mathbf{D}_\mathbf{r}^{-1}\mathbf{v}_\ell \\
=& \mathbf{D}_\mathbf{c}^{-1}(\mathbf{Z}-\mathbf{r}\mathbf{c}^\top)^\top\mathbf{D}_\mathbf{r}^{-1}\mathbf{u}_\ell \\
=& \mathbf{D}_\mathbf{c}^{-1}\mathbf{Z}^\top\mathbf{D}_\mathbf{r}^{-1}\mathbf{u}_\ell \\
=& \mathbf{C}\mathbf{D}_\mathbf{r}^{-1}\mathbf{u}_\ell \\
=& \mathbf{D}_\mathbf{c}^{-1}\mathbf{Z}^\top\mathbf{f}_\ell\delta_\ell^{-1},
\end{aligned} \tag{D.2}$$

where $\mathbf{C}$ is the column profiles where $\mathbf{C} = \mathbf{D}_\mathbf{c}^{-1}\mathbf{Z}^\top$ with each column of $\mathbf{C}$ sums to 1.

With sparsification, the new transition formulas for CA/MCA/DiSCA require the projecting operators used in

gsGSVD's algorithm:

$$
\begin{aligned}
\mathbf{f}_\ell &= \mathbf{D_r}^{-\frac{1}{2}} \operatorname{proj}_{\mathcal{L}_{\mathcal{G}_\mathbf{u}} \cap \mathcal{L}_2 \cap \mathbf{P}^\perp} \left(\mathbf{D_r}^{-\frac{1}{2}} \mathbf{X} \mathbf{g}_\ell \delta_\ell^{-1} \right) \delta_\ell \\
&= \mathbf{D_r}^{-\frac{1}{2}} \operatorname{proj}_{\mathcal{L}_{\mathcal{G}_\mathbf{u}} \cap \mathcal{L}_2 \cap \mathbf{P}^\perp} \left(\mathbf{D_r}^{-\frac{1}{2}} (\mathbf{Z} - \mathbf{r}\mathbf{c}^\top) \mathbf{g}_\ell \delta_\ell^{-1} \right) \delta_\ell \\
&= \mathbf{D_r}^{-\frac{1}{2}} \operatorname{proj}_{\mathcal{L}_{\mathcal{G}_\mathbf{u}} \cap \mathcal{L}_2 \cap \mathbf{P}^\perp} \left(\mathbf{D_r}^{-\frac{1}{2}} \mathbf{Z} \mathbf{g}_\ell \delta_\ell^{-1} \right) \delta_\ell \\
&= \mathbf{D_r}^{-\frac{1}{2}} \operatorname{proj}_{\mathcal{L}_{\mathcal{G}_\mathbf{u}} \cap \mathcal{L}_2 \cap \mathbf{P}^\perp} \left(\mathbf{D_r}^{-\frac{1}{2}} \mathbf{Z} \mathbf{g}_\ell \delta_\ell^{-1} \right) \delta_\ell \\
&= \mathbf{D_r}^{-\frac{1}{2}} \operatorname{proj}_{\mathcal{L}_{\mathcal{G}_\mathbf{u}} \cap \mathcal{L}_2 \cap \mathbf{P}^\perp} \left(\mathbf{D_r}^{\frac{1}{2}} \mathbf{R} \mathbf{v}_\ell \right) \delta_\ell,
\end{aligned}
\tag{D.3}
$$

and

$$
\begin{aligned}
\mathbf{g}_\ell &= \mathbf{D_c}^{-\frac{1}{2}} \operatorname{proj}_{\mathcal{L}_{\mathcal{G}_\mathbf{v}} \cap \mathcal{L}_2 \cap \mathbf{Q}^\perp} \left(\mathbf{D_c}^{-\frac{1}{2}} \mathbf{X}^\top \mathbf{f}_\ell \delta_\ell^{-1} \right) \delta_\ell \\
&= \mathbf{D_c}^{-\frac{1}{2}} \operatorname{proj}_{\mathcal{L}_{\mathcal{G}_\mathbf{v}} \cap \mathcal{L}_2 \cap \mathbf{Q}^\perp} \left(\mathbf{D_c}^{-\frac{1}{2}} (\mathbf{Z} - \mathbf{r}\mathbf{c}^\top)^\top \mathbf{f}_\ell \delta_\ell^{-1} \right) \delta_\ell \\
&= \mathbf{D_c}^{-\frac{1}{2}} \operatorname{proj}_{\mathcal{L}_{\mathcal{G}_\mathbf{v}} \cap \mathcal{L}_2 \cap \mathbf{Q}^\perp} \left(\mathbf{D_c}^{-\frac{1}{2}} \mathbf{Z}^\top \mathbf{f}_\ell \delta_\ell^{-1} \right) \delta_\ell \\
&= \mathbf{D_c}^{-\frac{1}{2}} \operatorname{proj}_{\mathcal{L}_{\mathcal{G}_\mathbf{v}} \cap \mathcal{L}_2 \cap \mathbf{Q}^\perp} \left(\mathbf{D_c}^{-\frac{1}{2}} \mathbf{Z}^\top \mathbf{f}_\ell \delta_\ell^{-1} \right) \delta_\ell \\
&= \mathbf{D_c}^{-\frac{1}{2}} \operatorname{proj}_{\mathcal{L}_{\mathcal{G}_\mathbf{v}} \cap \mathcal{L}_2 \cap \mathbf{Q}^\perp} \left(\mathbf{D_c}^{\frac{1}{2}} \mathbf{C} \mathbf{u}_\ell \right) \delta_\ell.
\end{aligned}
\tag{D.4}
$$

Appendix E. Simulated experiment to illustrate the loss of centering after projection

Barycentric projection is based on the property that, when data are (double) centered, any linear combination of the items will also be centered. Which makes factor scores and loadings also centered, when looking at the results of CA-related methods.

When sparsification is involved, however, this is no longer true, because the way that the components and loadings are obtained is not based on linear combinations anymore. However, there is one special case where this property holds again: when applying group-sparsification in the case of sparse MCA.

To observe this property on a simple simulated example, let's consider a normal random variable U, and $I = 100$ i.i.d. realisations of this random variable, stored into a vector $\mathbf{u}$. We then define the vector $\mathbf{x}$ of the centered values of $\mathbf{u}$ and $\mathbf{x}_{\mathcal{G}}$ the vector of the "group"-centered values of $\mathbf{u}$, where $\mathcal{G}$ defines a partition of $1, \cdots, I$ into 5 randomly assigned groups of 20. We then apply the projection operators $\text{proj}_{\mathcal{L}_1}$ and $\text{proj}_{\mathcal{L}_{\mathcal{G}}}$ on these two vectors with varying degrees of sparsity. The goal of this simulation is to visualize the effect of these projections on centered data, especially on the mean of the projected vectors, which is represented in Fig. E.6. We show on this plot the mean of the resulting projected vectors, as a function of the value of the sparsity parameter.

First, we see that projecting a centered vector on an $\mathcal{L}_1$- or an $\mathcal{L}_{\mathcal{G}}$-ball results in a vector that is sparser, but not centered anymore. However, when the input vector is group-centered, then the resulting (group-)projected vector is centered. This is due to the fact that the $\mathcal{L}_{\mathcal{G}}$-projection operator is scaling each group individually (therefore keeping each group centered) or eliminating them.

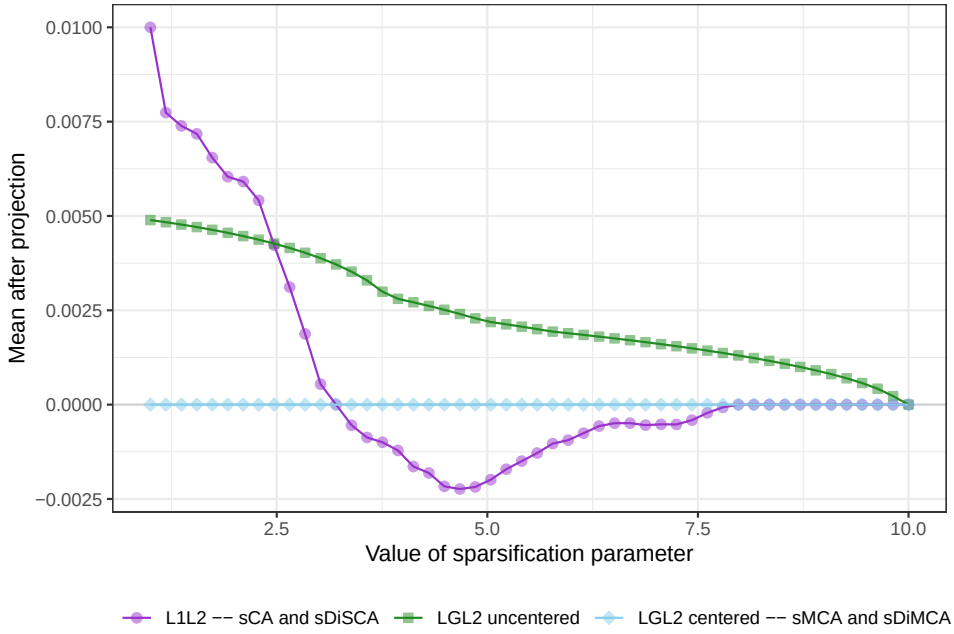

Figure E.6. Projections onto the $\mathcal{L}_1$- or $\mathcal{L}_{\mathcal{G}}$- ball of a centered vector does not usually yield centered vectors, except in the case of the $\mathcal{L}_{\mathcal{G}}$ projection of a group-centered vector. Although the means of projections onto $\mathcal{L}_1$- and $\mathcal{L}_2$-balls (colored in purple) crossed 0, the mean is not exactly, but only close to, 0 and does not satisfy the barycentric property.

Appendix F. Algorithms for plain SVD, GSVD, and sparse SVD (CSVD) and GSVD

Algorithm E.1: ALS algorithm of the SVD of $\mathbf{X}$

Data: $\mathbf{X}$, ε, R ▷ Data $\mathbf{X}$, errors ε, and rank R
Result: SVD of $\mathbf{X}$
$\mathbf{P} \leftarrow \emptyset$; $\mathbf{Q} \leftarrow \emptyset$ ▷ $\mathbf{P}$ and $\mathbf{Q}$ store the left and right singular vectors
for $\ell = 1, \ldots, R$ **do**
  Initialize $\mathbf{p}^{(0)}$ and $\mathbf{q}^{(0)}$ ▷ Initialize $\mathbf{p}$ and $\mathbf{q}$
  $\delta^{(0)} \leftarrow 0$; $\delta^{(1)} \leftarrow \mathbf{p}^{(0)\top}\mathbf{X}\mathbf{q}^{(0)}$ ▷ Update δ with $\mathbf{p}^{(0)}$ and $\mathbf{q}^{(0)}$
  $t \leftarrow 0$
  while $\left(\left\|\mathbf{p}^{(t+1)} - \mathbf{p}^{(t)}\right\|_2 \geq \varepsilon\right)$ or $\left(\left\|\mathbf{q}^{(t+1)} - \mathbf{q}^{(t)}\right\|_2 \geq \varepsilon\right)$ **do**
    $\mathbf{p}^{(t+1)} \leftarrow \mathbf{X}\mathbf{q}^{(t)}$
    $\mathbf{q}^{(t+1)} \leftarrow \mathbf{X}^\top\mathbf{p}^{(t+1)}$
    $\delta^{(t+1)} \leftarrow \mathbf{p}^{(t+1)\top}\mathbf{X}\mathbf{q}^{(t+1)}$
    $t \leftarrow t + 1$ ▷ Iterate until $\mathbf{p}$ and $\mathbf{q}$ are stable
  $\delta_\ell \leftarrow \delta^{(t)}$; $\mathbf{p}_\ell \leftarrow \mathbf{p}^{(t)}$; $\mathbf{q}_\ell \leftarrow \mathbf{q}^{(t)}$
  $\mathbf{P} \leftarrow [\,\mathbf{P} \mid \mathbf{p}_\ell\,]$
  $\mathbf{Q} \leftarrow [\,\mathbf{Q} \mid \mathbf{q}_\ell\,]$
  $\mathbf{X} \leftarrow \mathbf{X} - \delta_\ell \mathbf{p}_\ell^\top \mathbf{q}_\ell$

Algorithm E.2: ALS algorithm of the GSVD of $\mathbf{X}$

Data: $\mathbf{X}$, $\mathbf{M}$, $\mathbf{W}$, ε, R ▷ Data $\mathbf{X}$, row metric matrix $\mathbf{M}$, column metric matrix $\mathbf{W}$, error ε, and rank R
Result: GSVD of $\mathbf{X}$
$\widetilde{\mathbf{X}} = \mathbf{M}^{\frac{1}{2}}\mathbf{X}\mathbf{W}^{\frac{1}{2}}$
$\mathbf{U} \leftarrow \emptyset$; $\mathbf{V} \leftarrow \emptyset$ ▷ $\mathbf{U}$ and $\mathbf{V}$ store the *generalized* left and right singular vectors
for $\ell = 1, \ldots, R$ **do**
  Initialize $\mathbf{p}^{(0)}$ and $\mathbf{q}^{(0)}$ ▷ Initialize $\mathbf{p}$ and $\mathbf{q}$
  $\delta^{(0)} \leftarrow 0$; $\delta^{(1)} \leftarrow \mathbf{p}^{(0)\top}\widetilde{\mathbf{X}}\mathbf{q}^{(0)}$ ▷ Update δ with $\mathbf{p}^{(0)}$ and $\mathbf{q}^{(0)}$
  $t \leftarrow 0$
  while $\left(\left\|\mathbf{p}^{(t+1)} - \mathbf{p}^{(t)}\right\|_2 \geq \varepsilon\right)$ or $\left(\left\|\mathbf{q}^{(t+1)} - \mathbf{q}^{(t)}\right\|_2 \geq \varepsilon\right)$ **do**
    $\mathbf{p}^{(t+1)} \leftarrow \widetilde{\mathbf{X}}\mathbf{q}^{(t)}$
    $\mathbf{q}^{(t+1)} \leftarrow \widetilde{\mathbf{X}}^{\top}\mathbf{p}^{(t+1)}$
    $\delta^{(t+1)} \leftarrow \mathbf{p}^{(t+1)\top}\widetilde{\mathbf{X}}\mathbf{q}^{(t+1)}$
    $t \leftarrow t + 1$ ▷ Iterate until $\mathbf{p}$ and $\mathbf{q}$ are stable
  $\delta_\ell \leftarrow \delta^{(t)}$; $\mathbf{p}_\ell \leftarrow \mathbf{p}^{(t)}$; $\mathbf{q}_\ell \leftarrow \mathbf{q}^{(t)}$
  $\mathbf{u}_\ell \leftarrow \mathbf{M}^{-\frac{1}{2}}\mathbf{p}_\ell$
  $\mathbf{v}_\ell \leftarrow \mathbf{W}^{-\frac{1}{2}}\mathbf{q}_\ell$
  $\mathbf{U} \leftarrow [\mathbf{U} \mid \mathbf{u}_\ell]$
  $\mathbf{V} \leftarrow [\mathbf{V} \mid \mathbf{v}_\ell]$
  $\widetilde{\mathbf{X}} \leftarrow \widetilde{\mathbf{X}} - \delta_\ell \mathbf{p}_\ell^{\top}\mathbf{q}_\ell$

Note: The text colored in green is specific to the GSVD as compared to the SVD.

Algorithm E.3: ALS algorithm of the CSVD of $\mathbf{X}$

Data: $\mathbf{X}$, $s_{\mathbf{p},\ell}$, $s_{\mathbf{q},\ell}$, ε, R ▷ Data $\mathbf{X}$, errors ε, and rank R
▷ sparse parameters $s_{\mathbf{p},\ell}$ and $s_{\mathbf{q},\ell}$ for singular vectors
Result: CSVD of $\mathbf{X}$
$\mathbf{P} \leftarrow \emptyset$; $\mathbf{Q} \leftarrow \emptyset$ ▷ $\mathbf{P}$ and $\mathbf{Q}$ store the pseudo-left and right singular vectors
for $\ell = 1, \ldots, R$ **do**
  Initialize $\mathbf{p}^{(0)}$ and $\mathbf{q}^{(0)}$ ▷ Initialize $\mathbf{p}$ and $\mathbf{q}$ either from SVD or randomly
  $\delta^{(0)} \leftarrow 0$; $\delta^{(1)} \leftarrow \mathbf{p}^{(0)\top}\mathbf{X}\mathbf{q}^{(0)}$ ▷ Update δ with $\mathbf{p}^{(0)}$ and $\mathbf{q}^{(0)}$
  $t \leftarrow 0$
  while $\left(\left\|\mathbf{p}^{(t+1)} - \mathbf{p}^{(t)}\right\|_2 \geq \varepsilon\right)$ or $\left(\left\|\mathbf{q}^{(t+1)} - \mathbf{q}^{(t)}\right\|_2 \geq \varepsilon\right)$ **do**
    $\mathbf{p}^{(t+1)} \leftarrow \mathrm{proj}(\mathbf{X}\mathbf{q}^{(t)}, \mathscr{B}_{\mathcal{L}_2}(1) \cap \mathscr{B}_{\mathcal{L}_1}(s_{\mathbf{p},\ell}) \cap \mathbf{P}^{\perp})$ ▷ Projection of $\mathbf{X}\mathbf{q}^{(t)}$ onto the intersection
    $\mathbf{q}^{(t+1)} \leftarrow \mathrm{proj}(\mathbf{X}^{\top}\mathbf{p}^{(t+1)}, \mathscr{B}_{\mathcal{L}_2}(1) \cap \mathscr{B}_{\mathcal{L}_1}(s_{\mathbf{q},\ell}) \cap \mathbf{Q}^{\perp})$
    $\delta^{(t+1)} \leftarrow \mathbf{p}^{(t+1)\top}\mathbf{X}\mathbf{q}^{(t+1)}$
    $t \leftarrow t + 1$ ▷ Iterate until $\mathbf{p}$ and $\mathbf{q}$ are stable
  $\delta_\ell \leftarrow \delta^{(t)}$; $\mathbf{p}_\ell \leftarrow \mathbf{p}^{(t)}$; $\mathbf{q}_\ell \leftarrow \mathbf{q}^{(t)}$
  $\mathbf{P} \leftarrow [\mathbf{P} \mid \mathbf{p}_\ell]$
  $\mathbf{Q} \leftarrow [\mathbf{Q} \mid \mathbf{q}_\ell]$

Note: The text colored in red is specific to the CSVD as compared to the SVD.

Algorithm E.4: ALS algorithm of sGSVD of $\mathbf{X}$

Data: $\mathbf{X}$, $\mathbf{M}$, $\mathbf{W}$, $s_{\mathbf{p},\ell}$, $s_{\mathbf{q},\ell}$, ε, R

▷ Data $\mathbf{X}$, row metric matrix $\mathbf{M}$, column metric matrix $\mathbf{W}$, errors ε, and rank R

▷ sparse parameters $s_{\mathbf{p},\ell}$ and $s_{\mathbf{q},\ell}$ for singular vectors

Result: sGSVD of $\mathbf{X}$

$\widetilde{\mathbf{X}} = \mathbf{M}^{\frac{1}{2}}\mathbf{X}\mathbf{W}^{\frac{1}{2}}$

$\mathbf{U} \leftarrow \emptyset$; $\mathbf{V} \leftarrow \emptyset$ ▷ $\mathbf{U}$ and $\mathbf{V}$ store the pseudo-generalized left and right singular vectors

for $\ell = 1, \ldots, R$ **do**

  Initialize $\mathbf{p}^{(0)}$ and $\mathbf{q}^{(0)}$ ▷ Initialize $\mathbf{p}$ and $\mathbf{q}$ either from GSVD or randomly

  $\delta^{(0)} \leftarrow 0$; $\delta^{(1)} \leftarrow \mathbf{p}^{(0)\top}\widetilde{\mathbf{X}}\mathbf{q}^{(0)}$ ▷ Update δ with $\mathbf{p}^{(0)}$ and $\mathbf{q}^{(0)}$

  $t \leftarrow 0$ **while** $\left(\left\|\mathbf{p}^{(t+1)} - \mathbf{p}^{(t)}\right\|_2 \geq \varepsilon\right)$ or $\left(\left\|\mathbf{q}^{(t+1)} - \mathbf{q}^{(t)}\right\|_2 \geq \varepsilon\right)$ **do**

    $\mathbf{p}^{(t+1)} \leftarrow \text{proj}(\, \widetilde{\mathbf{X}}\mathbf{q}^{(t)}, \mathscr{B}_{\mathcal{L}_1}(s_{\mathbf{p},\ell}) \cap \mathscr{B}_{\mathcal{L}_2}(1) \cap \mathbf{P}^{\perp})$

    $\mathbf{q}^{(t+1)} \leftarrow \text{proj}(\, \widetilde{\mathbf{X}}^{\top}\mathbf{p}^{(t+1)}, \mathscr{B}_{\mathcal{L}_1}(s_{\mathbf{q},\ell}) \cap \mathscr{B}_{\mathcal{L}_2}(1) \cap \mathbf{Q}^{\perp})$

    $\delta^{(t+1)} \leftarrow \mathbf{p}^{(t+1)\top}\widetilde{\mathbf{X}}\mathbf{q}^{(t+1)}$

    $t \leftarrow t + 1$ ▷ Iterate until $\mathbf{p}$ and $\mathbf{q}$ are stable

  $\delta_\ell \leftarrow \delta^{(t)}$; $\mathbf{p}_\ell \leftarrow \mathbf{p}^{(t)}$; $\mathbf{q}_\ell \leftarrow \mathbf{q}^{(t)}$

  $\mathbf{u}_\ell \leftarrow \mathbf{M}^{-\frac{1}{2}}\mathbf{p}_\ell$

  $\mathbf{v}_\ell \leftarrow \mathbf{W}^{-\frac{1}{2}}\mathbf{q}_\ell$

  $\mathbf{U} \leftarrow [\,\mathbf{U} \mid \mathbf{u}_\ell\,]$

  $\mathbf{V} \leftarrow [\,\mathbf{V} \mid \mathbf{v}_\ell\,]$

Note: The text colored in red describes the sparsification constraints of the CSVD that are also used in the sGSVD, and the text colored in green describes the metric constraints of the GSVD that are also used in the sGSVD.

Appendix G. Supplementary Figures

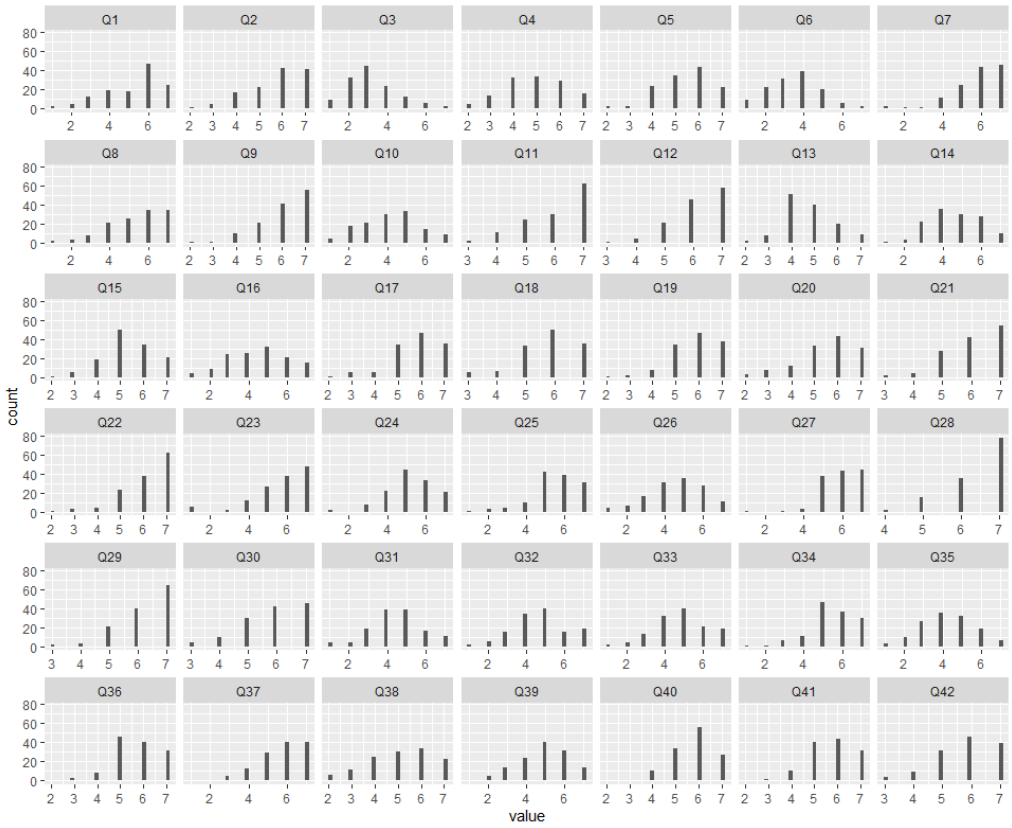

(a) The histogram of each item.

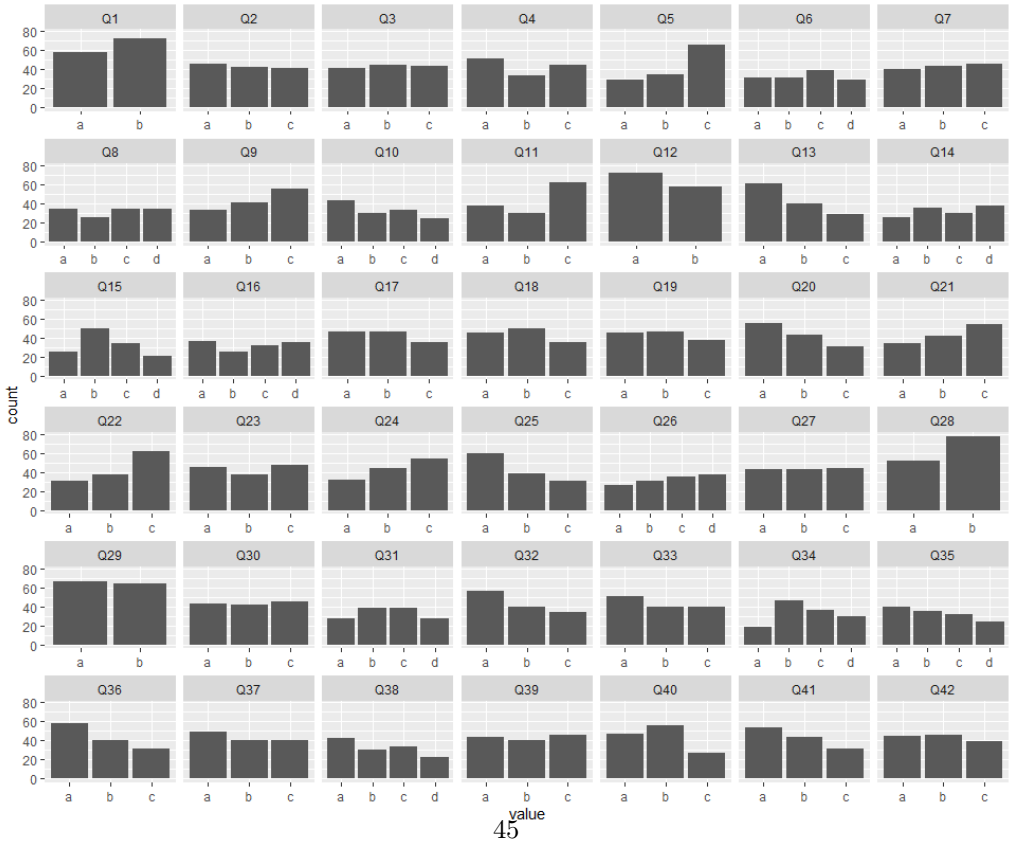

(b) The histogram of each item after binning.

Figure G.1. The grouping of item responses.

Figure G.2. Pattern of the associations between items. The items are grouped by hierarchical clustering analysis with minimized Ward distances.